resources

MDPI

Article

Molded Rigid Single-Use Containers from Cassava Residue, Sugarcane Bagasse, and Bacterial Cellulose Obtained from Low-Complexity Aqueous Processing

Cláudio José Galdino da Silva Junior [1,2,3,4], Anantcha Karla Lafaiete de Holanda Cavalcanti [3,5], Clécio José de Lacerda Lima [3,5], Italo José Batista Durval [3], Attilio Converti [3,6], Andréa Fernanda de Santana Costa [3,5] and Leonie Asfora Sarubbo [1,3,4,*]

1 Northeast Biotechnology Network (RENORBIO), Federal Rural University of Pernambuco (UFRPE), Rua Dom Manuel de Medeiros, s/n, Dois Irmãos, Recife 52171-900, Brazil; claudio.junior@iati.org.br
2 Northeast Biotechnology Network (RENORBIO), Federal University of Alagoas (UFAL), Av. Lourival Melo Mota, s/n, Tabuleiro do Martins, Maceió 57072-970, Brazil
3 Advanced Institute of Technology and Innovation (IATI), Rua Potyra, 31, Prado, Recife 50751-310, Brazil; anantchalafaiete@gmail.com (A.K.L.d.H.C.); clecio.lacerda@ufpe.br (C.J.d.L.L.); italo.durval@iati.org.br (I.J.B.D.); converti@unige.it (A.C.); andrea.costa@iati.org.br (A.F.d.S.C.)
4 School of Technology and Communication, Catholic University of Pernambuco (UNICAP), Rua do Príncipe, 526, Boa Vista, Recife 50050-900, Brazil
5 Center for Communication and Design, Academic Center of the Agreste Region, Federal University of Pernambuco (UFPE), BR 104, Km 59, s/n-Nova Caruaru, Caruaru 50670-90, Brazil
6 Department of Civil, Chemical and Environmental Engineering, University of Genoa (UNIGE), Pole of Chemical Engineering, Via Opera Pia, 15, 16145 Genoa, Italy
* Correspondence: leonie.sarubbo@unicap.br; Tel.: +55-81-21194084

Abstract

Agro-industrial waste-derived materials are promising candidates for short-cycle packaging applications. Here, we report a proof-of-concept for biodegradable biocomposites formulated with cassava residue (CR), sugarcane bagasse (SCB), and bacterial cellulose (BC) produced by symbiotic fermentation (SCOBY). This approach addresses the mechanical limitations typically associated with cassava starch-based matrices by introducing natural reinforcements to improve structural integrity and cohesion. A set of formulations with varying CR/BC/SCB ratios was processed and assessed through tensile and flexural testing, elongation at break, thermal analysis, and water-related behavior (sorption, absorption, and contact angle). Among the evaluated blends, formulation F1 (80% CR, 5% BC, 15% SCB) delivered the best overall balance between performance and moldability, achieving a tensile strength of 11.97 MPa and showing good dimensional stability. Biodegradability was confirmed by composting, reaching 72.74% mass loss after 84 days. Overall, BC incorporation improved matrix cohesion and enabled control of mechanical integrity and wettability in the blends, as highlighted for F1 (tensile strength 11.97 MPa; peak force 560.32 N; contact angle 65°; water absorption rate, WAR, 58.68%; sorption time 5.4 s). Given the abundance of sugarcane and cassava residues in Northeast Brazil, this low-complexity route leverages locally available feedstocks to add value to regional waste streams and support the partial replacement of synthetic polymers.

Keywords: biodegradable biocomposites; molded pulp packaging; water absorption; contact angle; soil biodegradation; circular bioeconomy

Academic Editor: Daniele Duca

Received: 9 February 2026
Revised: 11 March 2026
Accepted: 16 March 2026
Published: 17 March 2026

1. Introduction

The rapid growth in the use of disposable packaging and utensils has intensified the demand for non-biodegradable, fossil-based polymers (e.g., polystyrene and polypropylene), accelerating waste accumulation and the associated environmental and health risks. Global projections indicate that plastic consumption could rise from 464 Mt in 2020 to 884 Mt by 2050, with the accumulated stock potentially reaching up to 4725 Mt. Even under intervention scenarios, estimated plastic use in 2050 remains high, ranging from 594 to 1018 Mt. Sector-wide targets aiming at a 15% reduction by 2040 (relative to 2018) could lower plastic use in packaging by 27.3%, while achieving 55% recycling by 2030 could translate into more than 75% recycling of plastic packaging by 2050 [1]. In this context, sustainable and biodegradable polymers are a strategic option, though they face challenges related to scale, cost, performance, and waste-management infrastructure, requiring advances in materials science to accelerate adoption [2]. Among promising options, cellulosic/lignocellulosic platforms and bacterial cellulose are reported as lower-impact alternatives for packaging, with the potential for functional tuning through physicochemical modification and the use of agro-industrial residues, thus helping to reduce reliance on conventional polymers and their environmental impacts [3–6].

Agro-industrial residues are increasingly used as feedstock for moldable biodegradable biocomposites, with cassava (Manihot esculenta) standing out in Brazil due to its widespread distribution and economic importance. Cassava starch can be converted into biodegradable materials through simple methods (e.g., film formation/extrusion), adding value to existing production chains and supporting circular economy practices [7–9]. Quantitatively, films made from cassava waste starch have demonstrated antimicrobial activity with inhibition zones of 11.87 $\pm$ 1.62 mm, water vapor permeability of approximately 0.14 $g \cdot mm \cdot m^{-2} \cdot h^{-1} \cdot kPa^{-1}$, tensile strength around 0.17 MPa, and elongation at break about 32.9% [7]. Process intensification can further enhance performance: ozonation of cassava starch ($\approx$78.9 mg $O_3 \cdot g^{-1}$) resulted in a 43% increase in Young's modulus and a 37% decrease in hydrophobicity compared to native starch in extruded sheets [8]. From an implementation perspective in developing regions, the recent landscape includes 103 active patents and 379 publications (2022–2024) on starch-based flexible packaging, highlighting the importance of starch-based alternatives [10]. In this context, starch-only systems still face inherent limitations—brittleness, moisture sensitivity, and modest mechanical strength—that prevent large-scale adoption [10]; therefore, additives and blends such as glycerol (plasticizer) and chitosan (co-matrix) are often used to improve cohesion, flexibility, and barrier properties, increasing commercial viability [11,12].

Lignocellulosic waste like sugarcane bagasse (*Saccharum officinarum* L.), a by-product of Brazil's sugar–ethanol industry, offers fiber-rich reinforcement capable of enhancing the stiffness, strength, and dimensional stability of polymer matrices when properly processed or surface-modified [13]. Meanwhile, bacterial cellulose (BC), produced through symbiotic microbial fermentation, displays high crystallinity and purity, along with impressive water-holding capacity and mechanical performance compared to plant cellulose, while providing routes that avoid the harsher chemical processes typical of conventional pulping and bleaching [14–16].

While binary systems combining starch matrices with either macroscopic lignocellulosic fibers or nanocellulose have been explored, they often face distinct trade-offs. Binary blends of starch and macroscopic fibers (e.g., sugarcane bagasse) enhance bulk rigidity but typically exhibit poor interfacial adhesion, resulting in brittle composites with structural defects [17]. Conversely, binary blends of starch and bacterial cellulose offer excellent flexibility and cohesion but lack the required three-dimensional macroscopic stiffness for rigid packaging applications. Therefore, designing a ternary system integrating cassava residue

(CR), sugarcane bagasse (SCB), and bacterial cellulose (BC) offers a unique synergistic solution. In this ternary architecture, SCB provides the macroscopic structural backbone, CR acts as the bulk filler matrix, and BC functions as a highly crystalline, nanometric binder. The dense hydrogen-bonding network promoted by BC bridges the gap between the starch matrix and the rigid SCB fibers, effectively overcoming the brittleness of standard binary systems and yielding a cohesive, robust, and functional biocomposite [18,19].

In bagasse-based biocomposites, incorporating 30 wt% sugarcane bagasse into PLA results in an optimal combination of properties, including tensile strength of 31.78 MPa, tensile modulus of 219.49 MPa, and flexural strength of 53.25 MPa; increasing fiber content lowers the contact angle (from 83.2° in neat PLA to 32.3° at 50 wt% bagasse) and increases water absorption—effects that are reduced by inorganic fiber modification, which also boosts thermal stability ($\Delta T_i \approx +6.6$ °C) and crystallinity [20]. Additionally, sugarcane–bagasse/biobased composite systems demonstrate adjustable mechanical, thermal, and tribological properties under various formulations and processing conditions, consistent with the reinforcing role of lignocellulosic fibers [21]. The abundance and logistical accessibility of sugarcane co-products in Brazil further strengthen the case for residue-based material strategies in packaging applications [22].

As Brazil leads global sugarcane production (654.5 million tonnes in 2020/21) and ranks among the largest cassava producers, the valorization of these residues is a strategic pathway for materials development [22]. Here, we present a proof-of-concept biocomposite system that combines cassava residue and sugarcane bagasse with bacterial cellulose through simple, low-cost, aqueous processing, targeting sustainable disposable packaging. The innovation lies in the tri-component CR/SCB/BC architecture and the regionally sourced/processed strategy, which together enable improved cohesion, mechanical strength, and wettability control while maintaining biodegradability and compatibility with short-term uses. This approach addresses market demands for eco-friendly, technically strong alternatives to synthetic polymers and provides a practical route toward industrial scalability with low environmental impact, especially relevant to the bioeconomy of Northeastern Brazil

2. Materials and Methods

2.1. Microorganisms and Culture Medium

A symbiotic culture of bacteria and yeasts (SCOBY) was used for the synthesis of bacterial cellulose (BC). The microbial consortium was obtained from the culture bank of *Universidade Católica de Pernambuco* and composed mainly of lactic acid bacteria (*Lactobacillus* sp. and *Lactococcus* sp.), acetic acid bacteria (*Acetobacter* sp. and *Komagataeibacter hansenii*), and yeasts (*Saccharomyces cerevisiae*, *Zygosaccharomyces bailii*, and *Schizosaccharomyces pombe*), as described by Villarreal-Soto et al. [23]. The maintenance medium for development of the inoculum was composed of sucrose (50.0 g/L), a green tea infusion (10.0 g/L of *Camellia sinensis* leaves), and citric acid (1.15 g/L), with the pH adjusted to 6.0. It is important to note that the specific microbial composition of the symbiotic culture was not experimentally characterized in the present study (e.g., by genetic sequencing). Therefore, the microorganisms mentioned represent the typical microbiological profile widely established in the literature for standard Kombucha cultures, as extensively described by Villarreal-Soto et al. [23] and other previous studies.

2.2. Bacterial Cellulose Production, Purification, and Water Retention Capacity

For the production of BC, a 10% *v/v* pre-activated SCOBY culture was inoculated in rectangular glass vessels (capacity: 2.5 L) containing 2.0 L of sterilized green tea medium. Static fermentation was performed for 10 days at 30 °C, with the formation of cellulose

membranes at the air–liquid interface. The choice of a green tea–sucrose medium over the traditional Hestrin–Schramm (HS) medium offers significant advantages and can be supported by several reasons. Economically, HS medium depends on expensive analytical-grade reagents such as peptone, yeast extract, and pure glucose, which limits large-scale application. Conversely, commercial green tea and sucrose are readily available and inexpensive raw materials. Ecologically, this plant-based medium uses renewable, natural agricultural products instead of synthetic chemicals. Microbiologically, the symbiotic culture of bacteria and yeast (SCOBY) naturally thrives in this environment, quickly lowering the pH through organic acid production, which creates a self-protective environment against contaminating microorganisms—an essential factor for scaling up without strict sterile conditions. Finally, from an application perspective, using food-grade substrates ensures that the produced bacterial cellulose is completely safe, non-toxic, and highly suitable for creating sustainable packaging materials. The fermentation was carried out under static conditions with ambient oxygen, allowing aerobic bacteria to grow at the air–liquid interface and produce the BC pellicle. While continuous monitoring of parameters was not the focus here, typical fermentations using this protocol begin with an initial pH of around 5.0 to 4.0 (buffered by the starter liquid) and naturally decrease to a final pH of 3.0 due to organic acid accumulation. The membranes were rinsed in running tap water, then purified at 70 °C in 0.1 M NaOH for 1 h to remove microbial biomass. Following the alkaline treatment, the samples were subjected to multiple successive washing cycles with distilled water until the effluent reached a stable neutral pH, ensuring the complete removal of residual alkali and cellular debris. The wet mass was recorded to calculate the production yield [24,25]. Lastly, the membranes were weighed, and yields (g/L) were determined using Equation (1).

$$\text{Average yield}\left(\frac{\text{g}}{\text{L}}\right) = \frac{\text{Average BC mass (g)}}{\text{Average volume of production medium (L)}} \quad (1)$$

The water retention capacity (WRC) is a determinant for the integration of BC in hydrophilic matrices and is directly related to moisture content. The samples were dried in a laboratory oven at 50 °C for approximately 48 h until a constant weight was reached to ensure the elimination of residual moisture [26]. The WRC was estimated using Equation (2).

$$\text{WRC}(\%) = \frac{\text{Average wet BC mass (g)} - \text{Average dry BC mass (g)}}{\text{Average wet BC mass (g)}} \quad (2)$$

2.3. Preparation of Sugarcane Bagasse

Raw sugarcane bagasse (SCB) was submitted to manual pre-treatment to remove impurities. The treated material was ground in a knife mill to obtain fibrous particles. The biomass was dried for 12 h at 60 °C and then subjected to alkaline treatment with 3% NaOH at 80 °C for 2 h, using a recycled solution from the BC purification. This step was performed to remove lignin and residual impurities. The treated bagasse was washed until reaching neutral pH and stored in sealed containers [4]. Optimization of the alkaline pretreatment (i.e., comparison among different NaOH concentrations) was beyond the scope of the present study and will be addressed in subsequent work, including quantification of residual lignin and correlation with composite performance.

2.4. Preparation of Cassava Residue

Cassava residue (CR) was collected from the grinding and pressing stage of industrial starch extraction (cassava gum production). Although a specific proximate analysis of this batch was not conducted, cassava residue (commonly called cassava bagasse) from

this standard process is well documented in the literature as a hybrid biomaterial. Its dry matter typically consists mainly of residual starch (50–70%) and insoluble fibers (20–30%, primarily cellulose and hemicellulose), along with small amounts of proteins (~1.5%) and ash (~2.0%). This natural mixture of a thermoplastic component (starch) and a structural component (fibers) makes it an ideal base matrix for biocomposite formulation [27,28].

The material was then subjected to a standardized protocol to ensure stability, purity, and an adequate particle size for the formulation of biocomposites. CR was rinsed in running water to remove soil particles, sand, plant debris, and surface contaminants. The material was then spread in a thin layer of approximately 1 cm on perforated trays, followed by drying at 60 °C for 12 h in a forced-air oven to reduce free moisture and prevent fermentation and microbial degradation [29,30].

The dried material was ground in a knife mill to obtain fine powder with a uniform particle size compatible with the other components of the biocomposite matrix. The powder was then placed in an airtight container and stored in a desiccator containing silica gel as a desiccant, in a controlled environment (25 ± 2 °C) to prevent moisture reabsorption and preserve the material's physicochemical properties until application. This standardized preparation ensures reproducibility and consistency in the mechanical and processual performance of materials formulated with cassava residue.

2.5. Formulation of Biocomposites

The formulation of the biocomposites (Figure 1) was conducted to investigate the effect of composition on the physical–mechanical properties of materials intended for the production of sustainable packaging and disposable utensils. For this purpose, an experimental matrix composed of different proportions of cassava residue (CR), sugarcane bagasse (SCB), and bacterial cellulose (BC) was established. Each formulation was standardized to contain approximately 100 g of total solids, varying the relative percentages of the dry constituents according to the experimental design [4,31,32].

BC was synthesized through static fermentation using a symbiotic culture of bacteria and yeast (SCOBY), followed by purification and homogenization to obtain a cohesive fibrous paste (1800 rpm for 5 min in an industrial blender). The moistened, previously dried, and ground SCB was processed under the same conditions to promote partial disintegration of the lignocellulosic fibers. The two suspensions (BC and SCB) were mixed and further homogenized (1800 rpm for 5 min), resulting in a uniform appearance [4].

Cassava residue was manually incorporated into the mixture with a glass rod, gradually blending the components until a homogeneous, pasty mass was achieved. The mixture was then transferred to a hot plate and maintained at 90 °C under continuous manual stirring. The gelatinization of the cassava starch was visually identified by the formation of a viscous, sticky mass with characteristics of a moldable alloy. This thermal process was essential for promoting the cohesion of the natural polymer matrix.

Each sample received 1 mL of glycerin as a plasticizer to improve the malleability and structural cohesion of the final material. After complete homogenization, the masses were evenly distributed on glass or silicone plates and dried in a forced-air oven at 40 °C for 12 h until the plates were completely dry.

2.6. Mechanical and Physical Characterization

The mechanical and physical behavior of the biocomposites was assessed through tensile strength and repeated flexural testing. For the tensile analysis, rectangular specimens were cut from each formulation to standardized dimensions of 2.0 × 7.0 cm, with an average thickness of 1.5 mm. The tests were performed at room temperature (~25 °C) using a universal testing machine (BIOPDI, São Carlos, Brazil) equipped with a 5kN load cell. The

testing procedure followed an adapted methodology based on the ASTM D882 standard for thin plastic films and biopolymer sheets, with a crosshead speed of 50 mm/min. The variables of interest were maximum tensile strength at break (N), elongation at break (%), and Stress (MPa). Prior to tensile testing, the thickness of each specimen was measured using a digital micrometer. Dimensional uniformity was verified both visually, discarding samples with apparent macroscopic defects, and quantitatively, by taking multiple thickness readings along the gauge length of each specimen to ensure a consistent cross-sectional area.

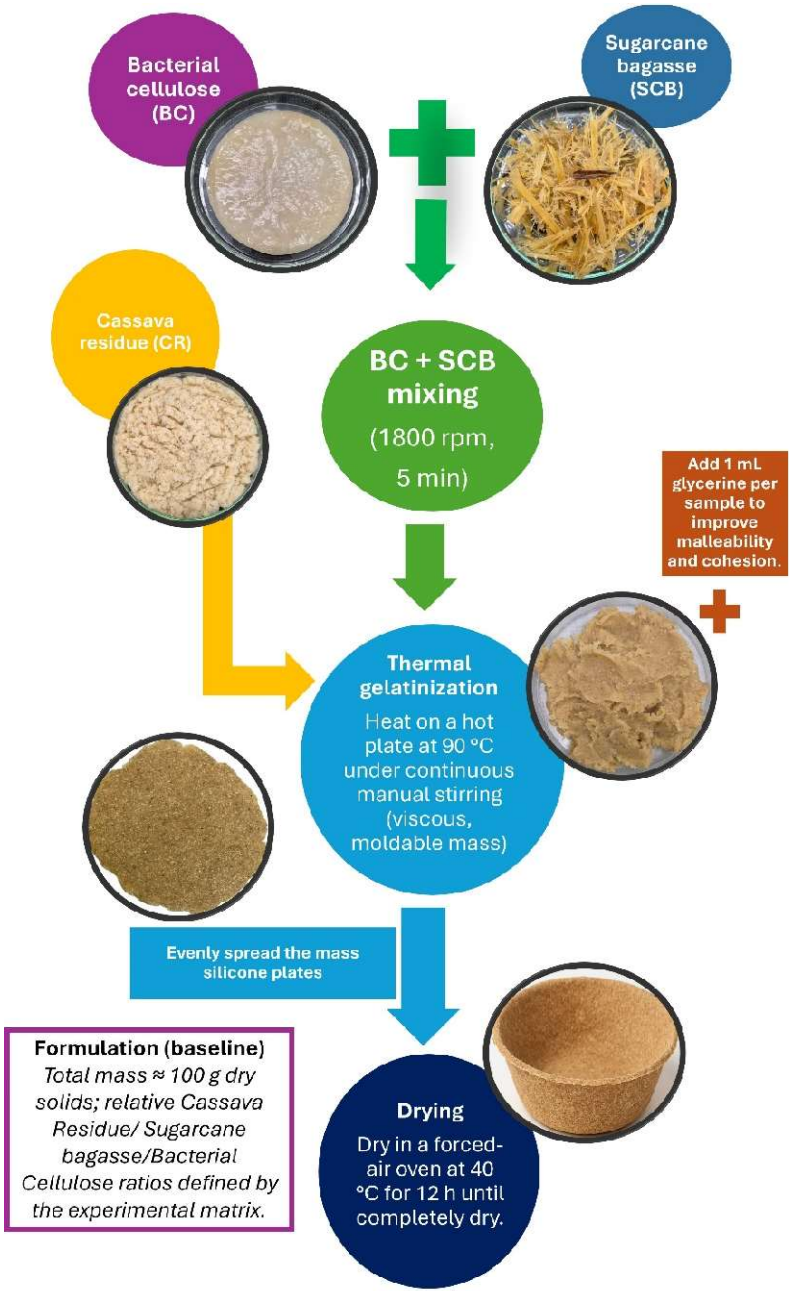

Figure 1. Preparation steps for cassava residue/sugarcane bagasse/bacterial cellulose biocomposites.

Flexural performance was investigated using a repeated manual bending test to simulate material fatigue under cyclic stress. Samples were bent back and forth along the same axis up to 100 times or until failure. Flexibility was qualitatively classified based on the number of successful bends without breaking, using the following scale adapted from [2]: poor (<20 bends), fair (20–49 bends), good (50–99 bends), and excellent (≥100 bends).

This procedure reflected the handling resilience expected in packaging and disposable applications, particularly for items subject to mechanical manipulation.

Together, these assessments provided insights into the structural integrity and durability of the different biocomposite formulations, serving as key criteria for selecting the optimal composition for further development and real-world applications.

2.7. Water Interaction Analyses

2.7.1. Contact Angle Measurement and Sorption Time

To investigate the surface wettability of the biocomposites, contact angle and water sorption time measurements were performed using the sessile drop method. Specimens (1 × 1 cm) were placed on a flat support to ensure a horizontal surface for droplet deposition. A ~25 µL drop of distilled water was carefully applied to the surface using a micropipette, and the contact angle (°) was recorded after 1.0 s using a digital camera (XT10, Fujifilm, Japan) mounted on a goniometer. This specific droplet volume was deliberately selected over smaller standard volumes (e.g., 5–10 µL) to account for the macroscopic surface roughness and structural heterogeneity of the bagasse-reinforced biocomposites. A larger droplet covers a broader surface area, preventing localized artifacts from individual exposed fibers or surface pores and thereby providing a more representative macroscopic contact angle. This rapid initial capture time was strictly necessary due to the extremely high hydrophilicity and porosity of the biocomposites, which caused the water droplets to be completely absorbed by the matrix within a few seconds, precluding accurate angle measurements at longer intervals (e.g., 10 s). To properly evaluate the dynamic wetting and absorption behavior, the total water sorption time (until complete droplet infiltration) was also continuously monitored and recorded. The procedure followed the guidelines established by Galdino et al. [33]. The droplet was observed for up to 10 min to determine the sorption time, defined as the total duration (in seconds) required for complete absorption of the water droplet into the material. The average time was calculated from triplicate measurements for each formulation.

2.7.2. Water Absorption Rate

To determine the water absorption rate of the biocomposite films, samples measuring 1 × 1 cm were dried, weighed (initial mass, m_0), and then immersed in 100 mL of distilled water at 37 °C for 24 h. After incubation, the hydrated samples were gently removed, blotted on silk-like absorbent paper to remove surface water, and immediately reweighed (wet mass, m_1). The water absorption rate (WAR, expressed as a percentage) was calculated using Equation (3):

$$\mathrm{WAR}(\%) = \frac{(m_1 - m_0)}{m_0} \times 100 \quad (3)$$

This test provided quantitative data on the hydrophilic behavior of the materials, which is critical for performance in food-contact and moisture-sensitive applications.

2.8. Biodegradability Assessment Under Simulated Composting Conditions

The biodegradability test was conducted in accordance with ISO 20200:2015—Plastics—Determination of the degree of disintegration of plastic materials under simulated composting conditions in a laboratory-scale test [34]. This method simulates aerobic composting conditions in a controlled laboratory environment and enables quantification of material disintegration by measuring mass over time.

For the composting matrix, a solid substrate was prepared with the following composition by weight: sawdust (40%), rabbit feed (30%), mature compost (10%), corn starch (10%), sucrose (5%), corn oil (4%), and urea (1%). The mixture was homogenized and placed in a

six-liter reactor, where the test specimens were embedded and maintained under stable composting conditions.

The total duration of the test was 90 days at a constant temperature of 58 °C, in line with ISO guidelines. Before and after the test, all samples were oven-dried at 40 °C to eliminate residual moisture and ensure accurate mass measurements. Three replicates of each formulation were tested. The specimens were visually inspected at intervals of 28, 56, and 84 days to monitor physical degradation.

The degree of disintegration (D, expressed as a percentage) was calculated based on the initial dry mass (m_i) and the final dry mass (m_f) after composting, according to Equation (4):

$$D(\%) = \frac{(m_i - m_f)}{m_i} \times 100 \quad (4)$$

This procedure enabled the quantitative analysis of the biodegradability of each formulation and supported comparative analysis between biocomposite variants under controlled composting conditions.

2.9. Thermogravimetric Analysis

To investigate the thermal stability of the biocomposites, thermogravimetric analysis (TGA) was performed using a simultaneous thermal analyzer (Shimadzu TGA-50) equipped with a platinum sample holder. Approximately 10 mg of each dried sample was placed in the crucible, and the measurement was conducted under an inert nitrogen atmosphere with a flow rate of 50 mL/min. The temperature range was from 25 °C to 800 °C, with a linear heating rate of 10 °C/min. This analysis provides critical insight into the applicability of the biocomposites in thermally demanding processes such as hot pressing and industrial molding [35,36].

2.10. Macroscopy

To investigate the surface morphology of the materials and understand the structural interactions among the components of the biocomposite, macroscopic analyses were performed using a 20×-80× binocular stereoscopic microscope (Olen®, ProWay Optics & Electronics LTD, Ningbo, China). BC, CR, SCB, and the F1 biocomposite (formulated with a combination of the three components) were analyzed. The materials were positioned on the support without dyes or fixatives and observed directly with transmitted light under an optical microscope (standard benchtop model). Images were captured with a camera coupled to the microscope and standardized for morphological comparisons.

2.11. Scanning Electron Microscopy (SEM)

To evaluate microstructural morphology, spatial uniformity, and physical interactions among the components (starch matrix, SCB, and BC), the formulation exhibiting the most favorable mechanical performance was selected for this analysis. Dried samples of the selected biocomposite were mounted on metal supports with conductive carbon tape and coated with gold for 30 s (SC-701 Quick Coater, Tokyo, Japan). The morphological analysis was performed using a scanning electron microscope (MIRA3 LM, Tescan, Warrendale, PA, USA).

2.12. X-Ray Diffractometry (XRD)

As with the morphological analysis, the biocomposite formulation exhibiting the most favorable mechanical performance was selected for X-ray diffraction (XRD). The crystallinity index (CrI) of this selected formulation and the bacterial cellulose (BC), along with the BC crystallite size, were evaluated using a D2 Phaser analytical diffractometer (Bruker, Billerica, MA, USA). The analysis was conducted with Cu Kα radiation generated

at 30 kV and 10 mA. Data were recorded in reflection mode over a scan range (2θ) from 5° to 80°, with an angular step of 0.05°. The CrI was determined using Equation (5):

$$\mathrm{CrI}(\%) = \frac{A_c}{A_c + A_{am}} \times 100 \quad (5)$$

where A_c is the area of the crystalline peaks, and A_{am} is the area of the amorphous halos. Peak deconvolution and area calculations were performed using Origin 8.5 software (OriginLab Corporation, Northampton, MA, USA).

2.13. Prototype Development

Based on mechanical performance and biodegradation results, formulation F1 (80% CR, 15% SCB, and 5% BC) was selected for prototyping. A circular container model was designed (12 cm in diameter at the top, 7 cm at the base, 3 cm in height, and wall thickness of 0.15 cm) and molded using a thermal press at 120 °C and 25 MPa for 10 min, simulating scalable industrial conditions. The dimensional stability and demolding capacity of the prototype were assessed qualitatively and photographically. The molding and processing conditions were selected based on the thermal and physical transitions of the biocomposite components. The initial thermal processing at approximately 90 °C was chosen to ensure temperatures well above the typical gelatinization range of cassava starch (60–75 °C), guaranteeing complete granular disruption and the formation of a cohesive viscoelastic matrix capable of thoroughly wetting the SCB fibers and BC network. For the curing stage, a moderate drying temperature of 40 °C was empirically selected. This controlled, low-temperature drying regime is crucial to prevent rapid moisture evaporation, thereby avoiding thermal stresses, warping, or surface cracking of the final rigid prototypes, ensuring stable dimensional retention after demolding.

3. Results and Discussion

3.1. Bacterial Cellulose Production

The average production of hydrated BC was 430.12 ± 17.92 g/L of fermentation medium, and the yield of dry BC was 14.02 ± 0.87 g/L, both after a 10-day cultivation period. These values indicate considerable production efficiency, especially when compared to data found in the literature. Adamopoulou et al. [37] and Thongsuk et al. [38] reported yields of 19.4 g/L and 13.44 g/L, respectively, for dry BC under static conditions over the same time interval. Galdino et al. [33] reported a yield of 422.12 ± 15.26 g/L for hydrated BC under static cultivation for 14 days, which is very close to the yield attained in the present investigation. Skaradziński et al. [39] reported a CB yield of 63.07 ± 2.91 g/L with a cultivation time of 295 h at a temperature of 28.0 °C.

The purification step with sodium hydroxide (NaOH) played a fundamental role in homogenizing the visual appearance of the BC by eliminating residual metabolites and possible impurities adhering to the biocellulose surface, as shown in Figure 2.

The BC employed here was produced using the same microbial consortium, under the same static-fermentation conditions, and using the identical alkaline purification workflow previously reported by Galdino et al. [4]. That study rigorously established the BC's composition and purity, confirming a cellulose structure and high chemical cleanliness after purification; therefore, the BC used in the present work conforms to the exact physicochemical specification.

Regarding water retention capacity (WRC), Table 1 shows that the BC had a retention rate greater than 96.0%. Bektas and Yildirim [40] reported a range of 150.0% to 177.7%. This high WRC is an essential property for the development of novel functional materials. The organization of cellulose fibers into three-dimensional networks confers desirable physical

characteristics to the material, such as high porosity and flexibility, and enhances the affinity of BC with hydrophilic materials.

Figure 2. Bacterial cellulose (BC) after purification process.

Table 1. Yield of bacterial cellulose (BC) after 10 days of cultivation and percentage of water retention capacity (WRC).

BC	Mean (g/L of Culture Medium) ± Standard Deviation	WRC (% *w*/*w*) ± Standard Deviation
Wet weight	430.12 ± 17.92	96.74 ± 0.23
Dry weight	14.02 ± 0.87	

Water plays a strategic role in BC's performance, contributing to its elasticity and mechanical strength by filling the spaces between cellulose fibers, enabling it to absorb moisture and expand without compromising its structural integrity—an essential quality for applications requiring durable, malleable materials [41]. Moreover, the high water content facilitates BC modification processes, including the incorporation of other hydrophilic materials, such as cassava and sugarcane bagasse, which are the focus of this study. This integration enables the composite's properties to be tailored to specific applications, such as the development of disposable products with greater strength and functional performance.

3.2. Development of Biocomposites

An experimental matrix was developed containing different biocomposite formulations with strategically selected proportions of bacterial cellulose (BC), sugarcane bagasse (SCB), and cassava residue (CR). The aim was to explore the synergy among the materials by observing the relative impact of each component on the properties of the final composite, in addition to prioritizing the most significant proportion of cassava, with BC and SCB serving as reinforcement materials. To facilitate identification and analysis, each formulation was coded with acronyms representing the proportions of its components. Table 2 presents these formulations, enabling a clear visualization of the proposed variations and serving as a basis for comparative physical and mechanical performance tests. Figure 3 shows the materials used in the biocomposite formulations.

Table 2. Formulations of biocomposites containing bacterial cellulose (BC), sugarcane bagasse (SCB), and cassava residue (CR).

Description	Biocomposites	Proportions (%)		
		CR	BC	SCB
CR-only (control)	F0	100	0	0
CR-major + BC 5% + SCB 15%	F1	80	5	15
CR-major + BC 10% + SCB 20%	F2	70	10	20
CR-major + BC 15% + SCB 25%	F3	60	15	25
CR/SCB balanced + BC 20%	F4	50	20	30
CR-major + BC 20% + SCB 15%	F5	65	20	15
CR-major + BC 10% + SCB 15%	F6	75	10	15
CR-minor + SCB 40% + BC 5%	F7	55	5	40
CR/SCB 60/40, no BC	F8	60	40	0
SCB-only (control)	F9	0	0	100
BC-only (control)	F10	0	100	0

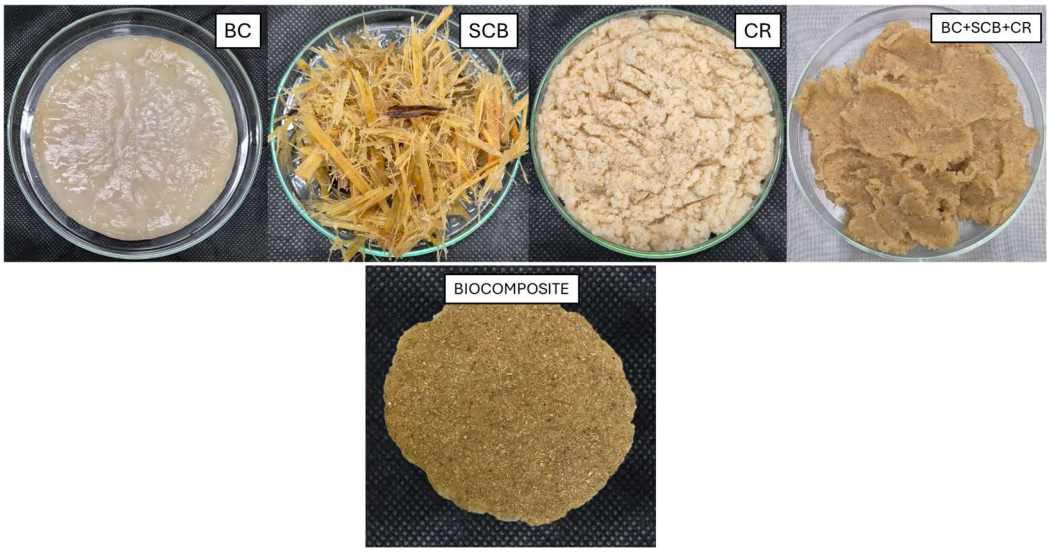

Figure 3. Visual aspects of bacterial cellulose (BC), sugarcane bagasse (SCB), cassava residue (CR), homogenized components (BC + SCB + CR), and biocomposite before drying.

The experimental design and the boundaries for the component ratios in the biocomposite formulations were logically determined based on the structural role of each material. Cassava residue (CR) was kept as the main continuous phase (≥70%) to guarantee enough thermoplastic starch for cohesive film formation. Sugarcane bagasse (SCB) was included as a micro-reinforcement up to a limit where macroscopic clumping and matrix damage are avoided. Conversely, the amount of bacterial cellulose (BC) was kept low (≤5%) to act as a nanoscale binder. This specific BC limit was determined by the percolation threshold for nanocellulose; maintaining low levels prevents excessive self-agglomeration through hydrogen bonding, thus ensuring even dispersion and optimal development of an interconnected 3D reinforcing network within the CR/SCB matrix.

The biocomposites had a visual appearance similar to that of a rigid plastic material, with a slightly rough surface, as shown in the images in Figure 4. For control and comparison purposes, single-component samples were produced containing exclusively one of the three materials in its pure form: cassava residue (CR), bacterial cellulose (BC), or sugarcane bagasse (SCB)—all used in full proportion (100%). Each of these samples exhibited visual and tactile properties consistent with the intrinsic characteristics of its respective material. The pure BC had a whitish color and a flexible texture, confirming

its versatility for applications in materials that require both flexibility and strength, as expected of the material in its pure form [42,43]. The samples composed solely of cassava residue exhibited an appearance and texture similar to those of commercially available biodegradable packaging, featuring uniformity and lightness. In contrast, the sugarcane bagasse composites had a brownish color and a rougher, more fibrous texture, resembling low-weight handmade paper and exhibiting a less cohesive fibrous structure.

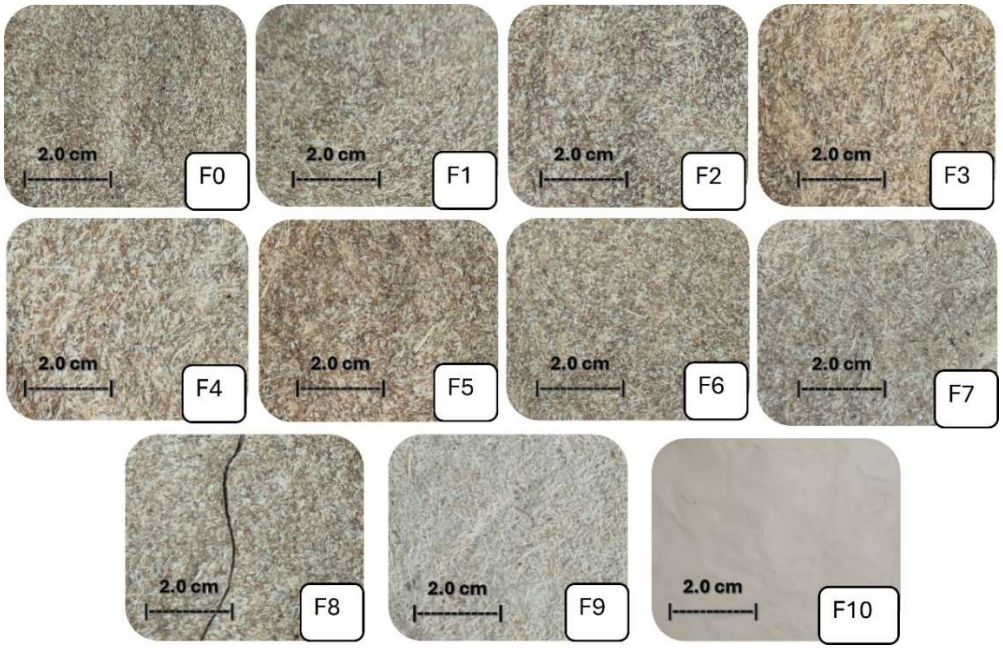

Figure 4. Visual aspect of biocomposites obtained from different formulations: F0 (100% cassava residue—CR), F1 (80% cassava residue—CR, 5% bacterial cellulose—BC, 15% sugarcane bagasse—SCB), F2 (70% cassava residue—CR, 10% bacterial cellulose—BC, 20% sugarcane bagasse—SCB), F3 (60% cassava residue—CR, 15% bacterial cellulose—BC, 25% sugarcane bagasse—SCB), F4 (50% CR, 20% bacterial cellulose—BC, 30% sugarcane bagasse—SCB), F5 (65% CR, 20% bacterial cellulose—BC, 15% sugarcane bagasse—SCB), F6 (75% cassava residue—CR, 10% bacterial cellulose—BC, 15% sugarcane bagasse—SCB), F7 (55% cassava residue—CR, 5% bacterial cellulose—BC, 40% sugarcane bagasse—SCB), F8 (60% cassava residue—CR, 40% bacterial cellulose—BC), F9 (100% sugarcane bagasse—SCB), F10 (100% bacterial cellulose—BC).

Obtaining biocomposites from the combination of BC, sugarcane bagasse, and cassava residue with cohesive structural characteristics constitutes an unprecedented advance in the literature. Although composites containing bacterial cellulose exist, the results confirm BC's ability to serve as a structural reinforcement material [44]. Its presence led to an apparent increase in the density and tactile stiffness of the composites, possibly by filling the interstitial spaces between the particles of the other components, thereby acting as a natural cohesive agent. This hypothesis will be tested in greater detail in the upcoming stages of physical and mechanical characterization. Another relevant point was the surface roughness of the composites with a higher proportion of sugarcane residue. This characteristic is considered undesirable for the proposed application (sustainable packaging with a good tactile finish) and indicates the need to adjust the final formulation or apply a surface treatment to improve the product's sensory appeal.

3.3. Contact Angle Measurement, Water Absorption Rate, and Sorption Time

Table 3 displays the contact angle (°), WAR (%), and sorption time (s) of the biocomposites developed. These data reflect the hydrophilic behavior of the samples when interacting with water and provide critical information for assessing their practical applicability.

Table 3. Contact angle (°), water absorption rate (WAR) (%), and sorption time (s) of biocomposites: F0 (100% cassava residue—CR), F1 (80% cassava residue—CR, 5% bacterial cellulose—BC, 15% sugarcane bagasse—SCB), F2 (70% cassava residue—CR, 10% bacterial cellulose—BC, 20% sugarcane bagasse—SCB), F3 (60% cassava residue—CR, 15% bacterial cellulose—BC, 25% sugarcane bagasse—SCB), F4 (50% CR, 20% bacterial cellulose—BC, 30% sugarcane bagasse—SCB), F5 (65% CR, 20% bacterial cellulose—BC, 15% sugarcane bagasse—SCB), F6 (75% cassava residue—CR, 10% bacterial cellulose—BC, 15% sugarcane bagasse—SCB), F7 (55% cassava residue—CR, 5% bacterial cellulose—BC, 40% sugarcane bagasse—SCB), F8 (60% cassava residue—CR, 40% bacterial cellulose—BC), F9 (100% sugarcane bagasse—SCB), F10 (100% bacterial cellulose—BC).

Biocomposite	Contact Angle (°)	WAR (%)	Sorption (s)
F0	12 ± 3	130.9 ± 6.41	1.35 ± 0.09
F1	65 ± 2	58.68 ± 2.33	5.4 ± 0.3
F2	58 ± 1	62.75 ± 2.11	3.7 ± 0.4
F3	60 ± 1	60.04 ± 1.34	5.5 ± 0.5
F4	56 ± 2	64.17 ± 0.33	7.8 ± 0.6
F5	70 ± 3	54.53 ± 3.32	2.1 ± 0.2
F6	61 ± 1	62.03 ± 1.12	3.3 ± 0.3
F7	58 ± 1	62.73 ± 0.22	6.9 ± 0.5
F8	65 ± 0,5	57.30 ± 0.75	1.8 ± 0.2
F9	39 ± 2	65.67 ± 0.27	77.32 ± 3.12
F10	15 ± 1	90.16 ± 0.29	0.78 ± 0.09

Table 3 highlights clear, data-supported trends in water–material interactions. The three single-component systems define the response range: F0 (100% cassava residue, CR) has the lowest contact angle and highest absorption (12 ± 3°; 130.9 ± 6.41%) with quick sorption (1.35 ± 0.09 s), aligning with highly wettable, starch-rich substrates noted in the literature [45]. F9 (100% bacterial cellulose, BC) shows moderate absorption (65.67 ± 0.27%) along with the longest sorption time (77.32 ± 3.12 s), consistent with BC's high water retention capacity [46]; and F10 (100% sugarcane bagasse, SCB) features a low contact angle (15 ± 1°) with rapid sorption (0.78 ± 0.09 s) and high absorption (90.16 ± 0.29%).

Among the blends, F1 (CR80/BC5/SCB15) offers the most balanced mix of wettability and uptake (65 ± 2°; 58.68 ± 2.33%; 5.4 ± 0.3 s), consistent with its overall performance elsewhere in the study. F5, F6, and F8 also demonstrate controlled uptake with short sorption times (F5: 54.53 ± 3.32%, 2.1 ± 0.2 s; F6: 62.03 ± 1.12%, 3.3 ± 0.3 s; F8: 57.30 ± 0.75%, 1.8 ± 0.2 s), while F4 and F7 show longer sorption times (7.8 ± 0.6 s and 6.9 ± 0.5 s, respectively) at similar contact angles (56–58°). Overall, higher contact angles tend to correlate with lower WAR (e.g., F5: 70 ± 3°; 54.53 ± 3.32%), whereas very low angles tend to correlate with higher uptake (e.g., F0: 12 ± 3°; 130.9 ± 6.41%). We note that porosity can influence these relationships (contact angle–uptake–sorption); although not measured here, pore structure will be quantified in future work to refine application-specific specifications.

For specific packaging applications where water resistance is crucial, implementing complementary waterproofing strategies is necessary [47]. Water resistance protects packaged products from moisture, ensuring their integrity and extending the shelf life [48,49]. Materials such as cellulose, despite being sustainable alternatives, exhibit hygroscopic behavior that leads to rapid water penetration, reducing mechanical properties under higher moisture conditions [47,50]. However, as the main objective in developing these biocomposites is to offer an environmentally friendly, biodegradable solution, the use of synthetic barriers or conventional plasticizers should be avoided.

A technically feasible, environmentally friendly solution would be the application of natural coatings based on waxes, such as carnauba wax or beeswax. These materials are biodegradable, well compatible with fibrous surfaces, and are already used in industry for

moisture control, gloss, and physical protection [51–53]. The application of these waxes by dipping, spraying, or fine brushing can form a hydrophobic surface barrier, significantly reducing water absorption without compromising the compostability of the final material. Moreover, the use of natural waxes can enable specific modulations, such as thermal resistance, antimicrobial properties (depending on the wax used), and extended product lifespans under real-life conditions [54,55]. Future studies should explore the effectiveness of these waxes at different concentrations and with varying application methods, and investigate their influence on the biodegradability and mechanical performance of composites.

3.4. Mechanical and Physical Characterization

Table 4 and Figure 5 display the results of the mechanical tests—maximum tensile strength, maximum stress, and elongation at break. The data demonstrates significant differences in performance among the formulations, reflecting structural interactions among the materials of the biocomposites with 1.5 mm (nominal thickness).

Table 4. Mechanical performance of 1.5 mm (nominal thickness) biocomposites: F0 (100% cassava residue—CR), F1 (80% cassava residue—CR, 5% bacterial cellulose—BC, 15% sugarcane bagasse—SCB), F2 (70% cassava residue—CR, 10% bacterial cellulose—BC, 20% sugarcane bagasse—SCB), F3 (60% cassava residue—CR, 15% bacterial cellulose—BC, 25% sugarcane bagasse—SCB), F4 (50% CR, 20% bacterial cellulose—BC, 30% sugarcane bagasse—SCB), F5 (65% CR, 20% bacterial cellulose—BC, 15% sugarcane bagasse—SCB), F6 (75% cassava residue—CR, 10% bacterial cellulose—BC, 15% sugarcane bagasse—SCB), F7 (55% cassava residue—CR, 5% bacterial cellulose—BC, 40% sugarcane bagasse—SCB), F8 (60% cassava residue—CR, 40% bacterial cellulose—BC), F9 (100% sugarcane bagasse—SCB), F10 (100% bacterial cellulose—BC).

Biocomposites	Strength (N)	Stress (MPa)	Elongation (%)	Apparent Density (g/cm^3)
F0	146.82 ± 4.97	3.14 ± 0.03	1.9 ± 0.04	0.71
F1	560.32 ± 7.66	11.97 ± 0.17	2.67 ± 0.03	1.07
F2	448.5 ± 5.71	9.58 ± 0.16	2.64 ± 0.04	0.96
F3	344.79 ± 8.51	7.37 ± 0.15	3.28 ± 0.04	0.84
F4	394.15 ± 7.03	8.42 ± 0.17	2.85 ± 0.07	0.76
F5	420.83 ± 12.2	8.99 ± 0.23	4.32 ± 0.11	1.04
F6	227.49 ± 2.52	4.86 ± 0.03	2.15 ± 0.01	1.00
F7	232.58 ± 1.01	4.97 ± 0.13	2.3 ± 0.01	0.83
F8	325.55± 4.93	4.75± 0.22	14.13 ± 0.71	0.76
F9	18.28 ± 0.91	0.39 ± 0.01	3.46 ± 0.14	0.29
F10	135.75 ± 5.39	2.9 ± 0.03	16.01 ± 0.54	0.43

The F1 formulation (80% CR, 5% BC, and 15% SCB) was the most mechanically resistant, with a tensile strength of 560.32 ± 7.66 N and a stress resistance of 11.97 ± 0.17 MPa. This superior performance can be attributed to the synergistic distribution of the reinforcing materials, with sugarcane bagasse contributing to stiffness and BC serving as a cohesive element promoting the continuity of the matrix [56]. Even with cassava residue as the significant component, the formulation preserved resistance, indicating that the presence of reinforcements in optimized proportions is more significant than their absolute predominance.

The F2, F4, and F5 formulations performed well, with stress resistance ranging from 8.42 to 9.58 MPa and tensile strength above 390 N. F5 combined satisfactory structural performance (8.99 ± 0.23 MPa) with high elongation (4.32 ± 0.11%), which makes it attractive for applications in which a balance is required between strength and malleability.

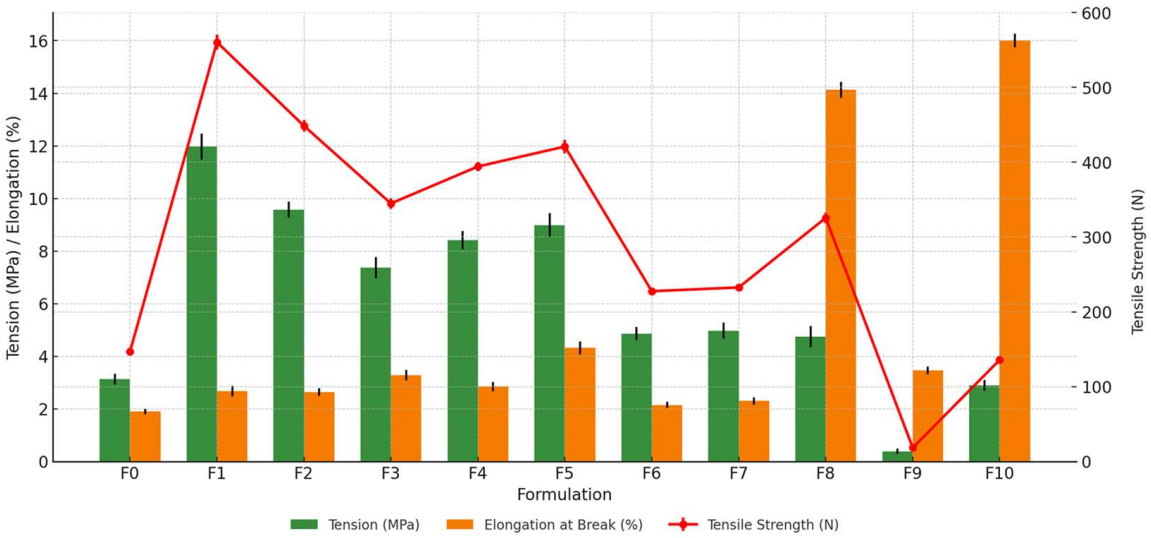

Figure 5. Mechanical performance of 15 mm (nominal thickness) biocomposites: F0 (100% cassava residue—CR), F1 (80% cassava residue—CR, 5% bacterial cellulose—BC, 15% sugarcane bagasse—SCB), F2 (70% cassava residue—CR, 10% bacterial cellulose—BC, 20% sugarcane bagasse—SCB), F3 (60% cassava residue—CR, 15% bacterial cellulose—BC, 25% sugarcane bagasse—SCB), F4 (50% CR, 20% bacterial cellulose—BC, 30% sugarcane bagasse—SCB), F5 (65% CR, 20% bacterial cellulose—BC, 15% sugarcane bagasse—SCB), F6 (75% cassava residue—CR, 10% bacterial cellulose—BC, 15% sugarcane bagasse—SCB), F7 (55% cassava residue—CR, 5% bacterial cellulose—BC, 40% sugarcane bagasse—SCB), F8 (60% cassava residue—CR, 40% bacterial cellulose—BC), F9 (100% sugarcane bagasse—SCB), F10 (100% bacterial cellulose—BC).

The F9 formulation (100% SCB) had the worst performance among all groups (18.28 ± 0.91 N and 0.39 ± 0.01 Mpa), demonstrating the structural fragility of sugarcane bagasse when used alone. Although fibrous, the lignocellulosic structure of bagasse is not cohesive enough to withstand tensile stress without an efficient binding agent. The F0 (pure CR) and F10 (pure BC) samples also had limitations. F0 was excessively stiff and brittle (3.14 MPa; 1.9% elongation), and F10 exhibited high ductility (16.01 ± 0.54%) but weak tension resistance (2.9 MPa). These findings indicate that none of the components alone offers an ideal mechanical performance, and the strategic combination among them is the key to developing adequate matrices.

The adaptive viscoelastic behavior of the mixed formulations is also noteworthy. For instance, F8 (60% CR, 40% BC, and 0% SCB) had the second-highest elongation at break (14.13 ± 0.71%), demonstrating the direct influence of BC on flexibility. Intermediate formulations, such as F3 and F6, showed moderate performance, revealing a transition between brittleness and ductility depending on the component balance.

BC proved to be an essential element for conferring flexibility and ductility, acting as a colloidal matrix (glue) that intertwines with the other constituents [56,57]. Sugarcane bagasse functioned as rigid reinforcement, which is essential for tensile strength, but its proportion must be controlled to avoid compromising cohesion [58]. Cassava residue (CR) contributed body and moldability but requires structural reinforcement to achieve satisfactory technical performance [59]. Bioplastics, such as those derived from CR, often have inferior mechanical properties compared to traditional plastics, limiting their application across various sectors [60,61].

To better understand the mechanical behavior, the apparent density of the biocomposites was measured (Table 4). The results show a notable macroscopic densification effect, especially in the optimized formulation (F1), which had an apparent density of 1.07 g/cm^3 compared to 0.71 g/cm^3 for the control (F0). This density increase indicates

a significant reduction in internal voids, caused by strong physical interactions and tight packing among the starch matrix, SCB, and BC fibers during drying. Hence, the improved mechanical performance seen in F1 is due to a highly synergistic effect: the macroscopic densification of the material (lower porosity) along with the microstructural reinforcement from the interconnected cellulosic network. This cohesive and uniform microstructure will be visually confirmed by the SEM images specifically obtained for the optimized F1 formulation, which are shown in the next section.

Therefore, the data suggest that formulations such as F1 are ideal for applications requiring high mechanical strength, such as utensils or structural packaging, while F4 and F5 are more versatile compositions balancing strength and flexibility. For applications requiring deformability and molding, formulations with a higher BC content, such as F8 and F10, may be preferable, provided they are reinforced or used in less demanding contexts.

Flexibility is a fundamental property for the functionality of biocomposites for packaging and disposable products, as it directly influences resistance to handling and deformation during use [62,63]. Among the formulations analyzed, F9 (100% BC) stood out for its high bending capacity, exceeding 100 cycles without breaking. This performance is associated with the nanofibrillar structure of BC, which provides elasticity, cohesion, and the efficient distribution of mechanical stress. F10 (100% SCB) performed significantly worse, breaking after only 22 cycles, reflecting the typical rigidity of lignocellulosic materials. Formulations composed exclusively or predominantly of CR (F0) did not withstand even one bending cycle, indicating structural fragility and low malleability. However, this rigidity can be beneficial in applications that require body and stability, such as trays or supports. The strategic addition of BC and sugarcane bagasse to the matrices, as in F1, F4, and F5, proved effective in increasing both strength and flexibility, demonstrating the usefulness of a hybrid approach for formulating biodegradable biocomposites with balanced mechanical performance.

3.5. Biodegradability Assessment Under Simulated Composting Conditions

Among the formulations developed, the F1 biocomposite (80% CR, 5% BC, and 15% SCB) was selected for biodegradability testing based on its superior performance in the mechanical tests and physicochemical analyses. This choice aimed to validate the environmental viability of the most promising formulation in terms of practical applications. Table 5 summarizes the data on the change in mass of the test specimens after the incubation period. Figure 6 visually illustrates the state of the samples at intervals of 0, 28, 56, and 84 days.

Table 5. Change in mass of F1 sample (80% cassava residue—CR, 5% bacterial cellulose—BC and 15% sugarcane bagasse—SCB) during biodegradability test.

Biocomposite	Test Specimen	Mass (g)	
		Initial	Final
F1 (CR-major + BC 5% + SCB 15%)	1	1.4881	0.2618
	2	1.5026	0.3445
	3	1.5606	0.6345
Mean		1.5171	0.4136
Standard deviation		0.0384	0.1957
Average change (%)		72.74	

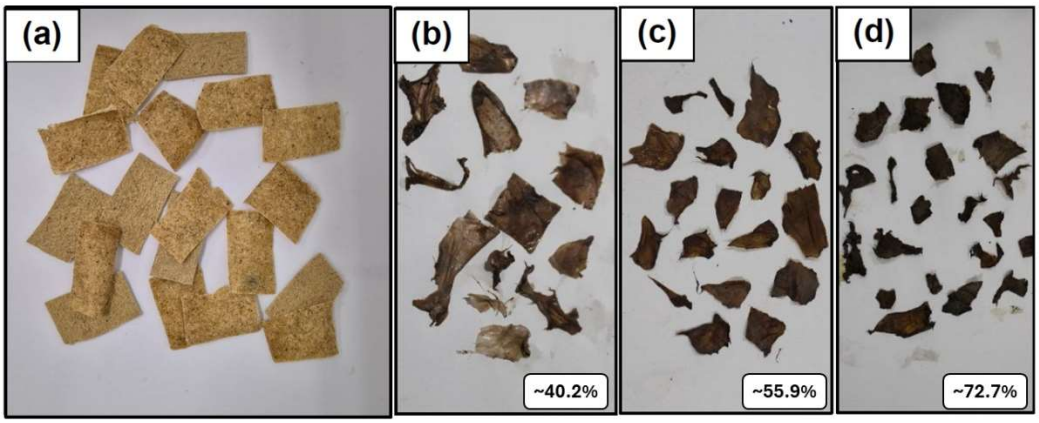

Figure 6. Results of biodegradability test with F1 sample (80% cassava residue—CR, 5% bacterial cellulose—BC, and 15% sugarcane bagasse—SCB): original on Day 0 (**a**); after 28 days (**b**); 56 days (**c**); 84 days (**d**).

At the end of the 84 days, the average reduction in mass was 72.74%, with individual variations ranging from 57% to 83%. The magnitude of this loss demonstrates an effective biodegradation process, confirmed by the progressive visual degradation of the samples over time. The presence of cracks, fragmentation, and structural collapse in the specimens indicates that the microorganisms in the compostable matrix degraded the starchy and cellulose fractions of the composite, demonstrating compatibility with natural decomposition processes.

The observed performance positioned the F1 biocomposite as a technically viable candidate for sustainable applications, combining good mechanical strength with biodegradability under controlled conditions. The disintegration rate was above the 70% threshold generally required for compostability certification, expanding the material's potential as a substitute for conventional plastics in short-cycle applications. A disintegration rate greater than 70% is an essential criterion for certifying the compostability of materials, as stipulated by standards such as ASTM D6400 and EN 13432, which establish the requirements for biodegradation, physical disintegration, and the absence of adverse ecotoxicological effects, ensuring that materials can be effectively decomposed in industrial composting facilities [64,65].

It is important to emphasize the synergistic relationship between the high water absorption capacity of the biocomposites and their rapid biodegradation rate. The initial phase of macroscopic breakdown is sped up by moisture-induced swelling, which physically disrupts the structural integrity of the highly hydrophilic starch matrix. However, instead of acting independently of biological activity, this physical swelling acts as a key facilitator of actual microbial degradation. The expansion of the polymer network increases the internal surface area and porosity, allowing soil moisture, colonizing microorganisms, and their secreted hydrolytic enzymes (such as amylases and cellulases) to penetrate deeply into the bulk of the composite. Therefore, although physical swelling starts the disintegration process, the ultimate mass loss—particularly the degradation of the more water-recalcitrant SCB and BC cellulosic fractions—is primarily driven by active microbial metabolism.

3.6. Thermogravimetric Analysis

Thermogravimetric analysis (TGA) was used to assess the thermal stability of the samples of bacterial cellulose (BC), sugarcane bagasse (SCB), cassava residue (CR), and the F1 biocomposite. The TGA and its derivative (DTG) curves (Figure 7) show distinct thermal behaviors among the materials, as summarized in Table 6.

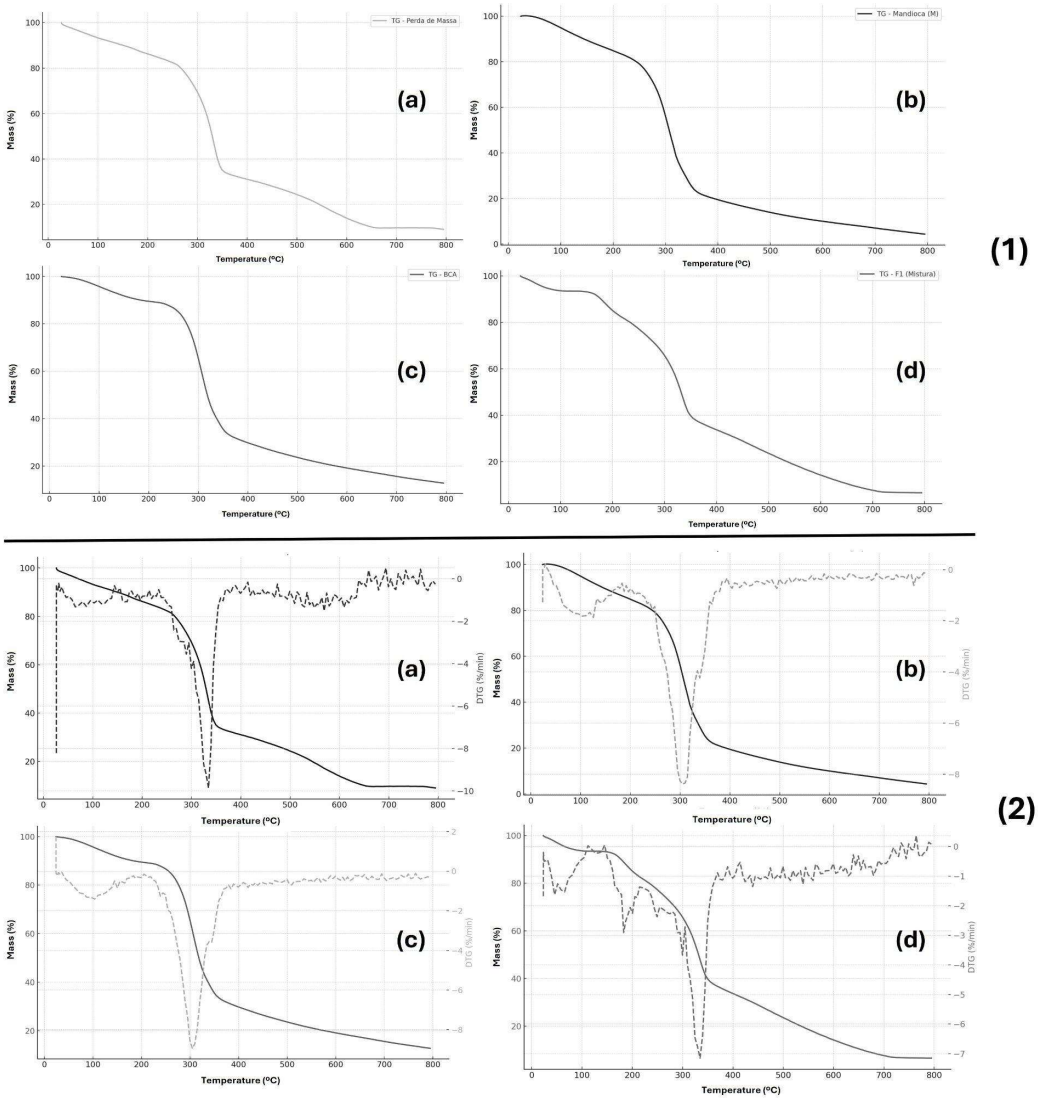

Figure 7. Thermogravimetric analysis (TGA) (1) and derivative thermogravimetric (DTG) (2) curves of bacterial cellulose (BC)—(**a**), cassava residue (CR)—(**b**), sugarcane bagasse (SCB)—(**c**), and the F1 biocomposite (80% cassava residue—CR, 5% bacterial cellulose—BC and 15% sugarcane bagasse—SCB)—(**d**).

Table 6. Characteristic temperatures and residual mass of bacterial cellulose (BC), cassava residue (CR), sugarcane bagasse (SCB), and the F1 biocomposite (80% cassava residue—CR, 5% bacterial cellulose—BC, and 15% sugarcane bagasse—SCB).

Sample	Initial Degradation Temperature (°C)	Peak DTG Degradation Temperature (°C)	Residual Mass (%)
CR	~220	~305	~4
BC	~260	~335	~8
SCB	~270	~330	~14
F1	255–260	325–335	~7

The earliest onset of degradation was found for the CR sample (~220 °C), indicating lower thermal stability. Mass loss was abrupt, peaking at ~305 °C, which is typical of starch-rich materials, whose amorphous structure favors pyrolysis at relatively low temperatures. The final residue (~4%) was the lowest among the formulations, suggesting nearly complete degradation.

The bacterial cellulose and sugarcane bagasse samples exhibited greater thermal stability. Degradation began above 260 °C in both samples, with multiple mass-loss events evident in the DTG curves. The main degradation peaks occurred between 330 and 340 °C, indicating the presence of more stable components, such as crystalline cellulose and possibly lignocellulosic compounds. The higher final residual mass of the sugarcane bagasse sample (~14%) may be attributed to the presence of anchored biomolecules or the formation of more refractory carbonaceous structures.

The F1 formulation, composed of cassava residue, bacterial cellulose, and sugarcane bagasse, exhibited an intermediate thermal profile, outperforming cassava residue alone. Degradation began between 255 and 260 °C, with peak mass loss at ~330 °C. The final residual mass (~7%) exceeded that of cassava and approached that obtained for BC. The broadening of the DTG curve and reduction in the maximum mass loss rate indicate synergistic behavior among the components of the biocomposite. These results may be explained by a barrier effect provided by the three-dimensional network of cellulose microfibres, which hinders the diffusion of heat and volatile products during pyrolysis. Furthermore, it is theoretically expected that intermolecular interactions, such as hydrogen bonds between the abundant hydroxyl groups of the starch matrix and cellulose fibers, may have contributed to the increased thermal stability of the system.

From a technological standpoint, the F1 formulation performed better than cassava residue alone, particularly due to its greater thermal stability and improved resistance to degradation. This thermal improvement, as evidenced by the increase in degradation temperature and final residual mass, was due to the enhanced mechanical properties previously demonstrated in this study. The synergistic combination of natural components with distinct decomposition profiles and reinforcing structures generally yields more robust functional biocomposites [66,67], as confirmed by TGA tests. Thus, F1 constitutes a technically more promising option for biodegradable packaging applications that require structural and thermal integrity, demonstrating its potential to replace conventional polymers in sustainable solutions.

In practical terms, the TGA/DTG profiles enable us to rank the thermal stability of the components and the composite (SCB ≈ BC > F1 > CR); to establish safe processing windows—our procedures (gelatinization/lamination at 90 °C and drying at 40 °C) are well below the degradation start points of F1 (255–260 °C), reducing the risk of thermal damage during manufacturing; and to guide post-processing decisions (e.g., thermal treatments, heat sealing, heat exposure) while maintaining safety margins below the 325–335 °C range (F1 DTG peak). Additionally, the final residue of F1 (~7%) falls between that of CR (~4%) and BC (~8%)/SCB (~14%), indicating an intermediate behavior consistent with the formulation and useful for screening heating processing routes. Therefore, TGA serves a diagnostic and predictive function by aligning thermal parameters for fabrication and use with the relative stability of the evaluated materials.

3.7. Optic Microscopic Analysis

Figure 8 shows images of the materials used individually (BC, CR, and SCB) and the resulting F1 biocomposite at magnification 40×, revealing the respective morphologies and degree of dispersion of the fibers in the final matrix.

The BC image reveals a dense, homogeneous, translucent structure with parallel nanofibril orientation and no visible fragments, confirming its purity and structural integrity. The cassava residue (CR) image reveals a heterogeneous morphology with particles of different sizes, predominantly starchy, and an irregular granular appearance, which can hinder uniform dispersion in the matrix without adequate treatment. The SCB image reveals a more extensive, intertwined fibrillar network with visibly long, aligned fibers,

characteristics of its lignocellulosic nature. This structure indicates its potential as a mechanical reinforcement for the biocomposite. The image of the F1 biocomposite shows the partial integration of the three components. The sugarcane fibers stand out for their length, promoting mechanical anchoring. BC serves as a structuring agent, providing cohesion between the particles, while CR acts as a filler matrix. These findings may explain the results obtained in the mechanical tests. However, the distribution of the components is somewhat heterogeneous, with visible clusters and spaces between fibers. This suggests that adjustments to the formulation or the homogenization stage could improve uniformity and the material's physical–mechanical performance.

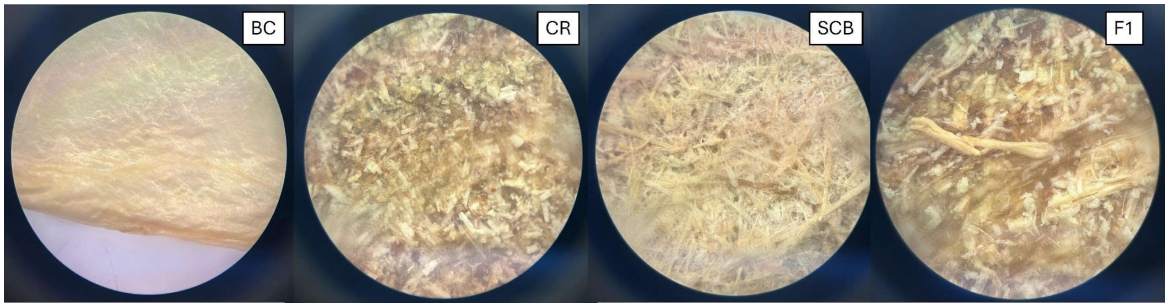

Figure 8. Images of individual constituents and F1 biocomposite (80% cassava residue—CR, 5% bacterial cellulose—BC and 15% sugarcane bagasse—SCB) obtained at a magnification of 40×: (BC) bacterial cellulose, (CR) cassava residue, (SCB) sugarcane bagasse, and (F1) final biocomposite.

Although optical microscopy provides qualitative information on the morphology of cassava residues, sugarcane bagasse, and bacterial cellulose, as well as on the apparent dispersion of fibers within the F1 matrix, it does not allow for the quantitative assessment of parameters such as fiber length, width, or fines content. Recent studies on molded pulp and plant-fiber systems utilize automated fiber analysis modules (e.g., MorFi) and high-resolution microscopy with dedicated software to establish more robust correlations between fiber structure and mechanical performance. Applying these approaches in future work is expected to deepen our understanding of the individual roles of CR, SCB, and BC in the structural response of the biocomposites.

3.8. Scanning Electron Microscopy (SEM)

To further examine the microstructural interactions and confirm the mechanical properties, Scanning Electron Microscopy (SEM) was used on the fractured surface of the optimized biocomposite formulation (F1) at various magnification levels. As shown in Figure 9, at lower magnifications (Figure 9a), the sample displays a highly uniform overall structure, indicating effective packing of the components with no visible phase separation. At higher magnifications (Figure 9b,c), the micrographs show fine, thread-like cellulosic structures forming a continuous and wavy network. Both the sugarcane bagasse (SCB) fibers and the bacterial cellulose (BC) are thoroughly embedded and evenly distributed within the thermoplastic starch matrix.

Notably, there is no significant fiber agglomeration, surface defects, or large voids. This microstructural integrity supports the apparent density results, indicating densification during drying. The strong interfacial adhesion between the cellulosic reinforcements and the starch matrix provides direct visual evidence of the enhanced mechanical properties of the F1 formulation. This cohesive interface prevents crack growth and allows efficient stress transfer from the softer starch matrix to the rigid SCB and BC network under load.

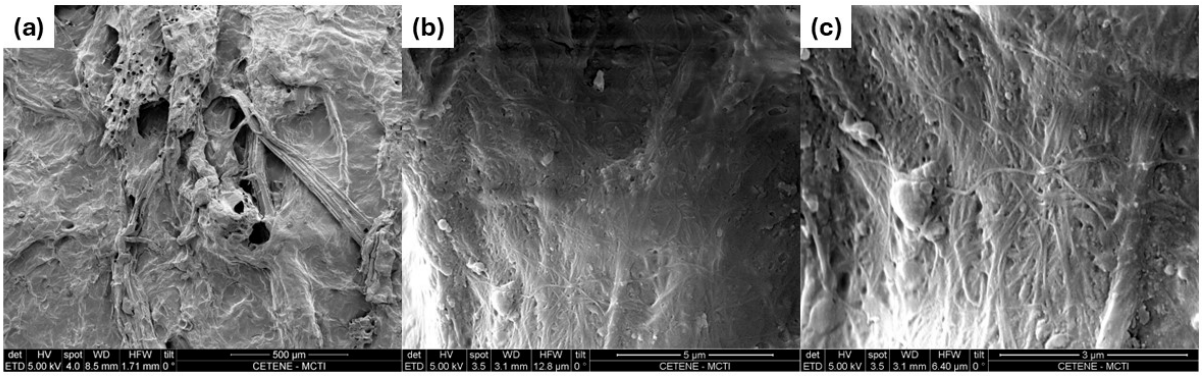

Figure 9. Scanning electron microscopy (SEM) micrographs of the fractured surface of the optimized biocomposite (F1) (80% cassava residue—CR, 5% bacterial cellulose—BC, and 15% sugarcane bagasse—SCB) at varying magnifications. Scale bars: (**a**) 500 μm, (**b**) 5 μm, and (**c**) 3 μm.

These microstructural findings align closely with recent research on hybrid cellulosic biocomposites. Santos and Spinacé [19] showed that combining thermoplastic starch with bacterial cellulose encourages extensive intermolecular hydrogen bonding, creating a tightly bound network that reduces internal porosity and boosts structural rigidity. Additionally, achieving a uniform dispersion of cellulosic reinforcements within starch matrices without significant agglomeration is widely regarded as a key factor for maximizing stress transfer and overcoming the typical brittleness of starch-based materials [17,68]. The effective physical entanglement seen in our SEM analysis confirms that the ternary combination in F1 successfully produced this synergistic structural reinforcement.

Overall, these microstructural observations provide the essential direct physical evidence to support the reinforcement mechanism proposed in this study. The visual confirmation of a tightly bound 3D cellulosic network, along with the absence of phase separation, definitively shows that the mechanical superiority of the F1 biocomposite is driven by the combined effects of macroscopic densification, uniform fiber distribution, and strong interfacial stress transfer.

3.9. X-Ray Diffractometry (XRD)

To better understand the structural properties and verify the reinforcement mechanism of the biocomposite at a molecular level, XRD analysis was conducted on the optimized F1 formulation.

The diffractogram of the F1 biocomposite (Figure 10) shows characteristic diffraction peaks at around 2θ = 14.6°, 17.0°, and 22.1°. These peaks mainly result from the crystalline regions of the cellulosic reinforcements (BC and SCB), specifically matching the typical crystallographic planes of cellulose type I. Meanwhile, the thermoplastic starch matrix mostly displays a more amorphous profile, with minor reflections near 2θ = 19.8°, which are typical of its structural changes during gelatinization and drying.

The calculated Crystallinity Index (CrI) for the F1 biocomposite was 38.7%. As widely reported in the literature, unreinforced thermoplastic starch, which forms the continuous matrix of this biocomposite, is almost entirely amorphous, usually showing near-zero crystallinity due to the complete disruption of its native granular structure during gelatinization. Conversely, pure bacterial cellulose (BC) displays a highly ordered crystalline structure with a CrI between 80% and 90% [69]. Therefore, achieving a CrI of 38.7% in the F1 formulation indicates a significant structural change, confirming a notable increase in crystallinity compared to a pure starch matrix. The presence of these crystalline domains demonstrates that the naturally high crystallinity of the BC and SCB fibers was effectively preserved during mixing and drying.

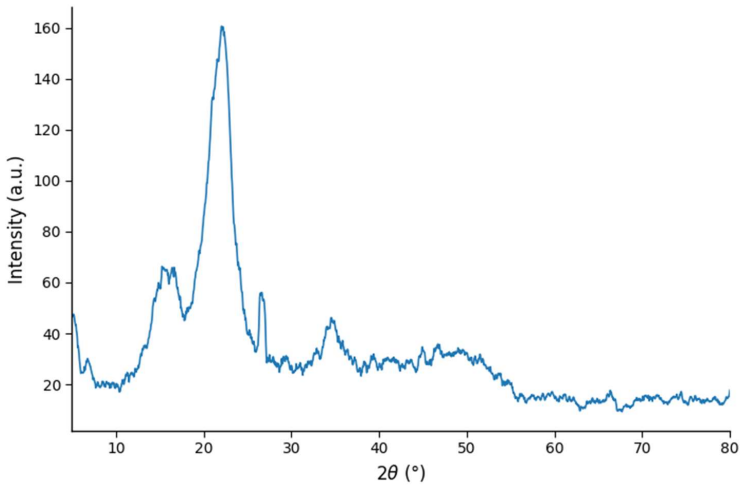

Figure 10. X-ray diffractograms of the pure bacterial cellulose (BC) and the optimized biocomposite formulation (F1) (80% cassava residue—CR, 5% bacterial cellulose—BC, and 15% sugarcane bagasse—SCB).

This structural characteristic is essential for the material's performance. The rigid crystalline regions of the cellulose network serve as physical anchors, limiting the movement of the amorphous starch chains. According to recent research on starch-based biocomposites, reaching an intermediate crystallinity level, such as the approximately 39% seen in F1, through nanocellulosic reinforcement is highly beneficial. This level provides an ideal balance, surpassing the inherent mechanical weakness of pure amorphous starch without causing excessive structural brittleness [18].

3.10. Prototype Development

Based on laboratory tests and the analysis of mechanical, thermal, hydrophilic, and structural properties, the F1 formulation was chosen as the most promising among the tested variants. F1 (CR80/BC5/SCB15) exhibited a tensile strength of 11.97 MPa, a contact angle of 65°, a water absorption rate (WAR) of 58.68%, and a sorption time of 5.4 s. Optical microscopy (40×) revealed a cohesive starch–cellulose network with fiber anchoring, and the plates demonstrated good bench-scale moldability during casting at 90 °C and maintained stable dimensions after drying at 40 °C, indicating suitability for rigid single-use packaging. Additionally, biodegradability was confirmed, with an average mass loss of 72.74% after 84 days in simulated composting conditions. Based on this selection, a geometric model of a disposable container with a circular base was designed, suitable for solid or semi-solid portions. Figure 11 displays a schematic drawing of the prototype with full-scale dimensions: a top diameter of 12 cm (mouth), a bottom diameter of 7 cm (base), a height of 3 cm, and a uniform wall thickness of 1.5 mm.

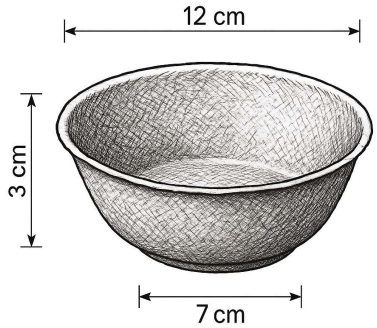

Figure 11. Design of biodegradable recipients in isometric cut with dimensional measurements (height, diameter of mouth, and diameter of base).

The material was then shaped using a concave mold under light thermal pressure and controlled drying. Figure 12 shows the biocomposite forming process in the plastic mold, revealing a homogeneous texture and uniform distribution of the components.

Figure 12. Molding step of biocomposite.

After molding and complete drying, the prototypes were analyzed for structural integrity and surface finish. Figure 13 shows the final container, which has an appearance compatible with sustainable plant-based products, sufficient rigidity for food storage, and easy handling.

Figure 13. Biodegradable recipient made from the F1 biocomposite (80% cassava residue—CR, 5% bacterial cellulose—BC, and 15% sugarcane bagasse—SCB).

During the molding and curing process, no macroscopic phase separation was observed between the aqueous starch matrix and the structural fibers. This high physical stability is attributed to the high viscosity of the fully gelatinized cassava starch combined with the exceptional water-holding capacity of the bacterial cellulose network. Regarding moisture dynamics, the material naturally showed an outside-in drying profile. Evaporation mainly occurred at the exposed surfaces, creating a moisture gradient that drove internal water outward through diffusion. The previously mentioned controlled drying temperature of 40 °C was essential to manage this moisture redistribution smoothly, preventing the formation of an impermeable outer crust and avoiding internal steam blistering or structural defects. Despite the satisfactory results, the molding stage posed a technical challenge. Demolding was difficult during the initial tests because of the material's adhesion to the mold and the piece's fragility before full drying. Figure 14 shows an example of a structural failure during one of the early attempts, where the prototype suffered irreversible

deformation and loss of shape. However, the material retained its mechanical strength, indicating that adjustments to the molding process and thermal parameters could enable scaled production.

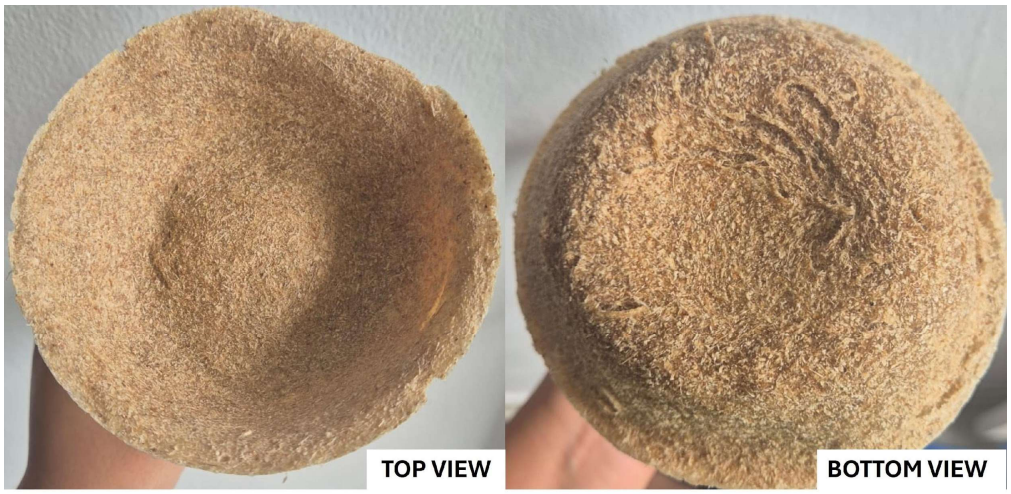

Figure 14. Preliminary demolding test with deformation of the prototype, demonstrating challenges in the standardization of the molding step involving the F1 biocomposite (80% cassava residue—CR, 5% bacterial cellulose—BC, and 15% sugarcane bagasse—SCB).

The mechanical value of F1 (CR80/BC5/SCB15) (11.97 MPa) falls within the upper range reported for cassava-starch films co-plasticized with honey or glycerol (about 9.41–20.35 MPa), even though our test pieces are rigid plates with a 1.5 mm wall thickness, not thin films. This order-of-magnitude similarity suggests that the three-component CR/BC/SCB composition creates an effective load-bearing network suitable for short-cycle rigid packaging, while Fernández et al. [70]'s films were optimized for flexibility and active functions (e.g., honey-assisted accelerated compostability).

In starch films containing Pickering emulsions stabilized by bacterial nanocellulose, the contact angle increased from 49.7° ± 1.5 to 71.0° ± 1.4, with a concurrent decrease in WVP from 0.085 ± 0.04 to 0.016 ± 0.01 $g \cdot mm \cdot h^{-1} \cdot m^{-2} \cdot kPa^{-1}$ (optimum at 2.5% *v/v* emulsion), without compromising strength. F1 shows 65° and WAR 58.68% with sorption at 5.4 s, placing it near that hydrophobicity range and indicating a direct pathway in surface/matrix engineering to reduce absorption/sorption without losing integrity—either via Pickering emulsions with BC-NF or low-mass natural coatings (e.g., waxes) [71].

It is also important to highlight evidence by Silveira et al. [7] on active cassava waste–starch films, which show antimicrobial activity with mean inhibition halos of 11.87 ± 1.62 mm, a water-vapor barrier around WVP ≈ 0.14 $g \cdot mm \cdot m^{-2} \cdot h^{-1} \cdot kPa^{-1}$, and typical thin-film mechanics ($\sigma_t \approx 0.17$ MPa; ε_b ≈ 32.9%). These data provide a quantitative benchmark for our system (F1: 65°, WAR = 58.68%; 5.4 s), indicating that Pickering emulsions/natural coatings can decrease absorption/sorption while maintaining integrity, whereas essential oils (e.g., clove) may add antimicrobial functionality when appropriate.

In starch foams reinforced with bacterial nanocellulose, a cell-nucleating effect and 2–3× increases in strength and modulus were observed (flexural ≈ 7.71 MPa; 448 MPa at 1.0 wt% NCF), along with a notable improvement in water resistance. These results reinforce the mechanism also observed in F1: BC acts as a cohesion and anchoring agent, and SCB provides fibrous reinforcement that stabilizes dimensions. In parallel, studies using chemically modified SCB (alkali/silane/acid) in thermoplastic matrices show reduced voids, better compatibility, and mechanical gains, in addition to tunable wettability—a promising route for F1's next cycle to lower WAR and adjust contact angle without sacrificing strength [72,73].

F1 achieved an average mass loss of 72.74% within 84 days of simulated composting, aligning with industrial disintegration standards. In comparison, honey-rich films reached approximately 80% in 100 days [70], highlighting that biodegradation can be sped up by hydrophilic additives and/or more open microstructures. Additionally, F1's thermal stability (TGA onset at 255–260 °C; DTG peak at 325–335 °C) remains well above the processing temperatures used here (90 °C/40 °C), allowing for thermal compression, heat sealing, and vacuum-assisted molding at a pilot scale. Overall, the data suggest F1 is a practical and modular option, with strength comparable to optimized films, intermediate wettability control, and proven compostability, while approaches such as Pickering strategies, natural coatings, and SCB modification offer concrete ways to improve barrier and moisture resistance to match or exceed current benchmarks in the literature. Although the developed prototype demonstrates promising mechanical properties and rapid biodegradability as an initial proof-of-concept, its highly hydrophilic nature poses challenges for extended shelf life. Long-term stability under varying humid storage conditions remains to be evaluated. Furthermore, transitioning this material to a commercial scale will require comprehensive testing to ensure compliance with strict industrial packaging performance standards (e.g., ASTM, ISO) and relevant government regulations. Future research will therefore focus on enhancing the prototype's moisture resistance and validating its performance and safety against these established normative requirements.

While the developed prototype demonstrates promising mechanical properties and rapid biodegradability, its highly hydrophilic nature poses challenges for extended shelf life. Long-term stability under varying humid storage conditions was not evaluated in this initial study and remains a critical next step. Future research will focus on assessing and potentially improving the prototype's moisture resistance during storage prior to its end-use application. It is important to emphasize that this prototype is an initial proof-of-concept. For future commercial scaling, the material must undergo comprehensive testing to comply with specific industrial packaging performance standards (e.g., ASTM, ISO) and strict government regulations, particularly concerning safety and long-term stability for specific end-use applications.

3.11. Rheological and Fiber-Structure Considerations: Limitations and Perspectives

From a rheological perspective, concentrated suspensions made from cassava residues, sugarcane bagasse, and bacterial cellulose tend to mimic the behavior of high-consistency lignocellulosic pastes previously described for bleached sugarcane bagasse pulps. Studies with bagasse suspensions at concentrations between 1.0 and 6.0 wt% fibers and temperatures between 20 and 60 °C, using a rheometer with a vane-in-cup geometry, show a strongly pseudoplastic behavior, with complex viscosity decreasing as shear rate increases. These findings reveal a significant dependence on consistency and viscoelastic moduli (G' and G''), which follow a power–law relationship with fiber concentration [74]. Practically, this means that small changes in solids content, fiber distribution, or degree of fibrillation can greatly influence paste flow during molding, affecting drainage, mold filling, and wall formation—aligning with the behavior seen in molded pulp systems as described in recent reviews [74,75].

The literature on fibers for molded pulp shows that rheological and forming properties are closely related to fiber structure, including chemical composition, average length, diameter, aspect ratio, fines content, and the presence of non-cellulosic components such as hemicelluloses, lignin, and pectins [75]. In sugarcane bagasse-based systems, comprehensive reviews indicate that this residue typically contains 32–45% cellulose, 20–32% hemicelluloses, 17–32% lignin, and 1–9% ash, along with extractives [76]. This lignocellulosic fraction, with high hemicellulose and moderate lignin content, promotes the

formation of a fiber network with good structural stiffness and a high specific surface area, which increases the yield stress and the resting viscosity of the suspensions [75,77]. Studies on molded pulp products further reveal that changing the fiber type, refining degree, and fines content can lead to significant variations in the mechanical strength, density, and water absorption of the final packages [76].

When considering cassava-processing residues, various studies indicate a hybrid nature, rich in both starch and fibers. Physicochemical characterization of cassava pulp and bagasse shows that the pulp contains about 50–70% starch (dry basis) and 20–30% fiber, mainly composed of cellulose and other non-starch polysaccharides [77]. Additional analyses report overall hemicellulose plus cellulose contents of around 34% and lignin contents close to 8% in cassava-processing residues [77]. Meanwhile, studies on extracting cellulose from cassava bagasse indicate that this by-product may contain approximately 15–50 wt% cellulosic fibers, depending on the origin of the raw material and pre-treatment conditions [78]. Collectively, these data support the view that cassava residue, in the formulation studied here, functions as a matrix rich in starch and hemicelluloses, with a significant fibrous component but lower lignin content compared to sugarcane bagasse [76–78].

From the perspective of nanoscale reinforcement, studies with nanocellulose derived from cassava bagasse show that crystallinity indices of about 84% can be achieved for cellulose nanocrystals, which are higher than the values reported for nanocellulose produced from commercial microcrystalline cellulose under similar conditions [79]. Research on cellulose nanofibrils extracted from cassava peels by mechanical defibrillation reports long nanofibrils with small diameters and zeta potentials lower than −47.7 mV, indicating high colloidal stability in aqueous media [79]. These results suggest that nanometer-scale cellulosic phases, such as those introduced by the bacterial cellulose used in this study, may serve as bridges between micrometric fibers, contributing to network cohesion and increasing the mechanical strength and wall integrity of the molded trays [75,77,78].

In this study, the experimental characterization was intentionally focused on dried biocomposites and the produced tray prototypes, emphasizing mechanical properties, water interaction (contact angle, absorption, and sorption kinetics), and biodegradation under simulated composting conditions. It also aimed to demonstrate the feasibility of bench-scale molding. Quantitative rheological tests on the suspensions—such as complete viscosity–shear-rate curves, experimental determination of yield stress, and oscillatory tests to obtain G' and G''—were not conducted, nor were automated analyses of fiber morphology (including length, diameter, fines content, and kink index) using fiber analysis modules. We acknowledge that the lack of detailed rheological and morphological data limits the ability to quantitatively describe paste microstructure and the connection between structure and the final tray properties. To address this limitation, we explicitly referenced available data from the literature on (i) rheology of sugarcane–bagasse suspensions [74], (ii) composition and structure of bagasse lignocellulosic fibers [76], (iii) composition and potential of cassava residues [77–79], and (iv) performance of commercial and experimental molded pulp products and biocomposites used for packaging [75,80,81], positioning our results within the current state of the art even without our own measurements of these parameters.

The mechanical results obtained for the CR/BC/SCB trays fall within a performance range consistent with values reported for molded pulp products used in food packaging. Recent reviews on fibers for molded pulp indicate that high-performance structural materials can achieve tensile strengths of up to around 17 MPa, depending on product density and fiber type [75]. Additionally, Liu et al. [80] describe tableware molded from mixtures of sugarcane bagasse and bamboo fibers with tensile strengths near 35 MPa, static contact

angles close to 127°, and predominant biodegradation under environmental conditions within approximately 60 days [80]. Biocomposites developed from residues of the cassava starch industry in a PHBV matrix demonstrate mechanical and barrier properties suitable for food packaging, reinforcing the potential of these residues as functional fillers in sustainable materials [81]. The combination observed in this study—mechanical strength adequate for packaging applications, high compostability, and the exclusive use of agro-industrial residues and bacterial cellulose—is therefore consistent with the performance range reported for similar materials in the literature [75,80,81].

Based on these results and the overview provided by existing literature, future research stemming from this study should include a dedicated stage of rheological and structural characterization of the ternary CR/BC/SCB suspensions. This can be achieved through (i) rotational and oscillatory rheometry within the consistency ranges used industrially for molded pulp [75,76], (ii) automated fiber analysis to measure fiber length, width, fines content, and kink index [75], and (iii) high-resolution microscopy combined with image analysis software to examine how fibers and starch/cellulose-rich phases are spatially distributed, and how this correlates with the mechanical and barrier properties of the final products. Incorporating these methods should enable, in future studies, the development of more direct links between fiber structure, paste rheology, and the in-use performance of the biocomposites. This approach will deepen scientific understanding and technological application, supplementing the data presented in this manuscript [74–81].

While the current study effectively demonstrates the macro-level mechanical handling and basic water resistance (absorption and solubility) of the developed biocomposites, some specific standardized metrics remain as areas for future development. For structural applications, quantitative flexural properties (e.g., standardized three- or four-point bending tests) will be necessary to complement the qualitative foldability screening conducted here. Additionally, for particular applications in primary food packaging, measuring the Water Vapor Transmission Rate (WVTR) is crucial and will be the focus of future development phases to fully scale this material for the food industry.

3.12. Scale-Up Perspectives and Economic Feasibility

Although the developed biocomposites require low processing complexity, scaling up to large-scale production presents specific economic challenges. According to our initial techno-economic estimates, the main cost driver is the biotechnological production of bacterial cellulose (BC). In this study, lab-scale production of dry BC costs around 125 USD per kilogram. For the optimized formulation (F1), even though BC makes up only 5% of the total dry weight, it accounts for nearly 97% of the direct raw material costs (estimated at approximately 6.40 USD per kg for the final biocomposite), since cassava residue and sugarcane bagasse are plentiful, virtually zero-cost agro-industrial wastes.

To overcome this economic barrier and move toward a sustainable circular economy model, large-scale production is planned to be integrated with commercial Kombucha beverage plants. In this mutually beneficial business model, the fermented beverage generates the main revenue, making the BC pellicle (often discarded as SCOBY—Symbiotic Culture of Bacteria and Yeast) a highly subsidized, value-added by-product [81]. Recent studies emphasize that using Kombucha-derived BC for sustainable materials significantly reduces biological synthesis costs [82].

Looking toward future industrial applications, scaling up bacterial cellulose (BC) production remains a recognized challenge. The main obstacles include the high cost of traditional fermentation media and the physical limitations of conventional scale-up methods, such as low productivity in static cultures and high shear stress in agitated bioreactors. However, emerging techniques are quickly progressing to increase BC yield and commer-

cial viability. These include using agro-industrial residues as low-cost alternative nutrient sources, implementing novel low-shear bioreactor designs (for example, rotary disk and airlift systems) to improve oxygen transfer, and employing specific culture additives that boost yield [83]. Combining these high-yield BC production strategies with the optimized agro-waste biocomposite formulation (F1) developed in this study offers a highly promising and cost-effective path for scalable manufacturing of sustainable packaging.

From a life cycle perspective, this integrated approach simplifies the environmental footprint. It reduces the environmental impact of agro-waste disposal, operates under low-energy processing conditions (compared to synthetic polymer extrusion), and produces a 100% compostable product. As a result, combining biocomposite manufacturing with beverage production not only makes the final biodegradable packaging economically viable but also strongly supports the principles of the bioeconomy and the Sustainable Development Goals (SDGs), especially responsible consumption and production (SDG 12) and climate action (SDG 13).

4. Conclusions

This proof-of-concept study shows that agro-industrial residues—cassava residue (CR), sugarcane bagasse (SCB), and bacterial cellulose (BC)—can be combined using a simple aqueous process to produce moldable, biodegradable biocomposites suitable for short-term packaging. Among the tested variants, F1 (CR80/BC5/SCB15) provided the most balanced performance, with a tensile strength of 11.97 MPa, a contact angle of 65°, a WAR of 58.68%, a sorption time of 5.4 s, and a 72.74% mass loss after 84 days under simulated composting conditions. TGA revealed a safe processing window (onset at 255–260 °C; DTG peak at 325–335 °C), well above the low-temperature manufacturing parameters used here (90 °C casting; 40 °C drying). Prototype trays with 1.5 mm wall thickness confirmed bench-scale moldability and dimensional stability at the laboratory scale.

At the scientific level, this work establishes an initial link between the composition and fiber architecture of CR/BC/SCB systems and their macroscopic mechanical, water interaction, and compostability behaviors. Technically, the tri-component CR/BC/SCB structure enhances matrix cohesion and fiber anchoring while remaining biodegradable, making it suitable for rigid single-use containers. The findings align with market demands for lower-impact materials and are strategically important in regions where CR and SCB are plentiful (e.g., Northeast Brazil), adding value to underused residue streams and supporting circular bioeconomy goals.

The research will now develop along three main areas: (i) performance optimization using bio-based surface barriers (such as natural waxes) and/or Pickering emulsions to further decrease water uptake and sorption; (ii) more detailed characterization, including porosity, water-vapor and oxygen barriers, dynamic mechanical analysis, rheological behavior of high-consistency CR/BC/SCB suspensions, fiber morphology, and structure–property relationships; and (iii) scaling efforts, with heat-/vacuum-assisted compression molding, demolding improvements, and manufacturing consistency. These steps will refine specifications, enable application-specific designs (for dry versus moist foods), and support future techno-economic and life-cycle assessments for industrial use.

5. Patent

The innovation resulting from this research has been filed for intellectual property protection under the Brazilian National Institute of Industrial Property (INPI) with the following title and protocol:

"Biodegradable Biocomposite Based on Cassava Residue, Sugarcane Bagasse, and Bacterial Cellulose for Sustainable Packaging", protocol number BR102025015356-4, filed on 24 July 2025.

The patented technology refers to a mouldable, compostable biocomposite composed of renewable feedstock and agro-industrial waste. The formulation comprises 60–70% cassava residue, 10–20% processed sugarcane bagasse, and 10–30% purified bacterial cellulose, and includes a manufacturing process involving drying, grinding, microbial fermentation, cellulose purification, and molding. This biocomposite holds potential for industrial-scale applications and technology transfer in the packaging, food, and cosmetics sectors.

Author Contributions: Conceptualization, C.J.G.d.S.J., A.K.L.d.H.C., A.F.d.S.C. and L.A.S.; methodology, C.J.G.d.S.J.; validation, C.J.G.d.S.J. and L.A.S.; formal analysis, I.J.B.D., C.J.d.L.L. and C.J.G.d.S.J.; investigation, C.J.G.d.S.J. and A.K.L.d.H.C.; writing—original draft preparation, C.J.G.d.S.J., I.J.B.D., L.A.S. and A.K.L.d.H.C.; writing—review and editing, C.J.d.L.L., A.F.d.S.C., A.C. and L.A.S.; visualization, C.J.G.d.S.J., A.C. and L.A.S.; supervision, L.A.S.; project administration, C.J.G.d.S.J. and L.A.S.; funding acquisition, A.C. and L.A.S. All authors have read and agreed to the published version of the manuscript.

Funding: This study was funded by the Brazilian development agencies Coordenação de Aperfeiçoamento de Pessoal de Nível Superior (CAPES, Finance Code 001), Fundação de Apoio à Ciência e Tecnologia do Estado de Pernambuco (FACEPE), and Conselho Nacional de Desenvolvimento Científico e Tecnológico (CNPq).

Institutional Review Board Statement: Not applicable.

Informed Consent Statement: Not applicable.

Data Availability Statement: The original contributions presented in the study are included in the article; further inquiries can be directed to the corresponding author.

Acknowledgments: The authors are grateful to the Northeast Biotechnology Network (RENORBIO), Federal Rural University of Pernambuco (UFRPE), Federal University of Alagoas (UFAL), Coordenação de Aperfeiçoamento de Pessoal de Nível Superior (CAPES), Federal University of Pernambuco (UFPE), the Catholic University of Pernambuco (UNICAP), the Advanced Institute of Technology and Innovation (IATI), Fundação de Apoio à Ciência e Tecnologia do Estado de Pernambuco (FACEPE), and Conselho Nacional de Desenvolvimento Científico e Tecnológico (CNPq).

Conflicts of Interest: The authors declare no conflicts of interest.

References

1. Dokl, M.; Copot, A.; Krajnc, D.; Fan, Y.V.; Vujanović, A.; Aviso, K.B.; Tan, R.R.; Kravanja, Z.; Čuček, L. Global projections of plastic use, end-of-life fate and potential changes in consumption, reduction, recycling and replacement with bioplastics to 2050. *Sustain. Prod. Consum.* **2024**, *51*, 498–518. [CrossRef]
2. Teixeira, S.C.; de Oliveira, T.V.; Soares, N.F.F.; Raymundo-Pereira, P.A. Sustainable and biodegradable polymer packaging: Perspectives, challenges, and opportunities. *Food Chem.* **2025**, *470*, 142652. [CrossRef]
3. Thomas, P.; Kayarkatte, N. Eco-conscious consumption. In *Eco-Innovation and Sustainable Development in Industry 5.0*; Advances in Logistics, Operations, and Management Science Book Series; IGI Global Scientific Publishing: Hershey, PA, USA, 2024; pp. 1–26. [CrossRef]
4. da Silva Junior, C.J.G.; de Medeiros, A.D.M.; Cavalcanti, A.K.L.d.H.; de Amorim, J.D.P.; Durval, I.J.B.; Cavalcanti, Y.d.F.; Converti, A.; Costa, A.F.d.S.; Sarubbo, L.A. Towards sustainable packaging using microbial cellulose and sugarcane (*Saccharum officinarum* L.) bagasse. *Materials* **2024**, *17*, 3732. [CrossRef]
5. Hong, Y. Study on the maximum level of disposable plastic product waste. *Sustainability* **2023**, *15*, 9360. [CrossRef]
6. Saroha, R.; Bathla, G.; Kumar, H.; Sharma, G. Towards waste minimization in food packaging. In *Global Sustainable Practices in Gastronomic Tourism; Advances in Hospitality, Tourism and the Services Industry (AHTSI)*; IGI Global Scientific Publishing: Hershey, PA, USA, 2024; pp. 191–204. [CrossRef]

7. Silveira, Y.D.O.; Franca, A.S.; Oliveira, L.S. Cassava waste starch as a source of bioplastics: Development of a polymeric film with antimicrobial properties. *Foods* **2025**, *14*, 113. [CrossRef]
8. Lafuente, C.; Siqueira, L.; Augusto, P.; Tadini, C. Bio-based plastic based on ozonated cassava starch produced by extrusion. *J. Polym. Environ.* **2022**, *30*, 3974–3984. [CrossRef]
9. Lilavanichakul, A.; Yoksan, R. Development of bioplastics from cassava toward the sustainability of cassava value chain in Thailand. *Sustainability* **2023**, *15*, 14713. [CrossRef]
10. Garavito, J.; Peña-Venegas, C.P.; Castellanos, D.A. Production of starch-based flexible food packaging in developing countries: Analysis of the processes, challenges, and requirements. *Foods* **2024**, *13*, 4096. [CrossRef]
11. Kusumawati, R.; Syamdidi; Abdullah, A.H.D.; Nissa, R.C.; Firdiana, B.; Handayani, R.; Munifah, I.; Dewi, F.R.; Basmal, J.; Wibowo, S. Physical properties of biodegradable chitosan-cassava starch based bioplastic film mechanics. *Sci. Technol. Indones.* **2025**, *10*, 191–200. [CrossRef]
12. Dodino-Duarte, I.; Quiroz-Ortega, L.; Arias-Benítez, J.C.; García-León, R.A. Development of biodegradable plastic films from cassava starch. *Dyna* **2024**, *91*, 75–85. [CrossRef]
13. Etuk, S.; Agbasi, O.; Robert, U. Investigation of heat transfer and mechanical properties of Saccharum officinarum leaf board. *Int. J. Energy Water Resour.* **2021**, *6*, 95–102. [CrossRef]
14. Płoska, J.; Garbowska, M.; Pluta, A.; Stasiak-Różańska, L. Bacterial celulose: Innovative biopolymer and possibilities of its applications in dairy industry. *Int. Dairy J.* **2023**, *140*, 105586. [CrossRef]
15. Singh, A.K.; Chandra, R. Pollutants released from the pulp paper industry: Aquatic toxicity and their health hazards. *Aquat. Toxicol.* **2019**, *211*, 202–216. [CrossRef]
16. Andriani, D.; Apriyana, A.Y.; Karina, M. The optimization of bacterial cellulose production and its applications: A review. *Cellulose* **2020**, *27*, 6747–6766. [CrossRef]
17. Sapuan, S.M.; Harussani, M.M.; Ismail, A.H.; Soh, N.S.Z.; Azwardi, M.I.M.; Siddiqui, V.U. Development of nanocellulose fiber reinforced starch biopolymer composites: A review. *Phys. Sci. Rev.* **2024**, *9*, 1171–1211. [CrossRef]
18. Csiszár, E.; Kun, D.; Fekete, E. The Role of structure and interactions in thermoplastic starch–nanocellulose composites. *Polymers* **2021**, *13*, 3186. [CrossRef]
19. Santos, T.A.; Spinacé, M.A.S. Sandwich panel biocomposite of thermoplastic corn starch and bacterial cellulose. *Int. J. Biol. Macromol.* **2021**, *167*, 358–368. [CrossRef] [PubMed]
20. Peng, Y.; Lei, W.; Yu, W.; Chen, Y. Effect of sugarcane bagasse content and modification on the properties of sugarcane bagasse/poly(lactic acid) biocomposites. *Molecules* **2025**, *30*, 1583. [CrossRef]
21. Samanth, M.; Hiremath, P.; Deepak, G.D.; Naik, N.; H S, A.; Heckadka, S.S.; Shivamurthy, R.C. Sustainable composites from sugarcane bagasse fibers and bio-based epoxy with insights into wear performance, thermal stability, and machine learning predictive modeling. *J. Compos. Sci.* **2025**, *9*, 124. [CrossRef]
22. Angelo, J.; Oliveira, M.; Ghobril, C. Balança comercial dos agronegócios paulista e brasileiro de 2020. *Análises E Indicadores Do Agronegócio* **2021**, *16*, 1–16.
23. Villarreal-Soto, S.A.; Beaufort, S.; Bouajila, J.; Souchard, J.; Taillandier, P. Understanding kombucha tea fermentation: A review. *J. Food Sci.* **2018**, *83*, 580–588. [CrossRef]
24. Treviño-Garza, M.Z.; Guerrero-Medina, A.S.; González-Sánchez, R.A.; García-Gómez, C.; Guzmán-Velasco, A.; Báez-González, J.G.; Márquez-Reyes, J.M. Production of microbial cellulose films from green tea (*Camellia sinensis*) kombucha with various carbon sources. *Coatings* **2020**, *10*, 1132. [CrossRef]
25. Charoenrak, S.; Charumanee, S.; Sirisa-ard, P.; Bovonsombut, S.; Kumdhitiahutsawakul, L.; Kiatkarun, S.; Pathom-Aree, W.; Chitov, T.; Bovonsombut, S. Nanobacterial cellulose from kombucha fermentation as a potential protective carrier of *Lactobacillus plantarum* under simulated gastrointestinal tract conditions. *Polymers* **2023**, *15*, 1356. [CrossRef]
26. Bodea, I.M.; Beteg, F.I.; Pop, C.R.; David, A.P.; Dudescu, M.C.; Vilău, C.; Stănilă, A.; Rotar, A.M.; Cătunescu, G.M. Optimization of moist and oven-dried bacterial cellulose production for functional properties. *Polymers* **2021**, *13*, 2088. [CrossRef]
27. Andrade, L.R.S.; Felisardo, R.J.A.; Cruz, I.A.; Bilal, M.; Iqbal, H.M.N.; Mulla, S.I.; Bharagava, R.N.; Souza, R.L.; Azevedo, L.C.B.; Ferreira, L.F.R. Integrated Biorefinery and Life cycle assessment of cassava processing residue–from production to sustainable evaluation. *Plants* **2022**, *11*, 3577. [CrossRef]
28. Drummond, F.R.; Cardoso, P.H.M.; Anaya-Mancipe, J.M.; Thiré, R.M.S.M. Biocomposites of starch industry residues from cassava and poly(3-hydroxybutyrate-co-3-hydroxyvalerate) for food packaging. *Processes* **2025**, *13*, 719. [CrossRef]
29. Ribeiro, T.S.M.; Martins, C.C.N.; Scatolino, M.V.; Dias, M.C.; Mascarenhas, A.R.P.; Ferreira, C.B.; Bianchi, M.L.; Tonoli, G.H.D. Using cellulose nanofibril from sugarcane bagasse as an eco-friendly ductile reinforcement in starch films for packaging. *Sustainability* **2025**, *17*, 4128. [CrossRef]
30. Veiga, J.P.S.; Valle, T.; Feltran, J.C.; Bizzo, W.A. Characterization and productivity of cassava waste and its use as an energy source. *Renew. Energy* **2016**, *93*, 691–699. [CrossRef]

31. Serpa-Fajardo, J.G.; Hernández-Ramos, E.J.; Andrade-Pizarro, R.D.; Aguilar-Lasserre, A.A.; Fernández-Lambert, G. Innovation in cassava bagasse valorization: Efficiency of convective drying enhanced with ultrasound and pulsed electric fields. *Foods* **2024**, *13*, 2796. [CrossRef] [PubMed]
32. Jeencham, R.; Chiaoketwit, N.; Numpaisal, P.-o.; Ruksakulpiwat, Y. Study of Biocomposite Films based on cassava starch and microcrystalline cellulose derived from cassava pulp for potential medical packaging applications. *Appl. Sci.* **2024**, *14*, 4242. [CrossRef]
33. Junior, C.J.G.d.S.; de Amorim, J.D.P.; de Medeiros, A.D.M.; Cavalcanti, A.K.L.d.H.; Nascimento, H.A.D.; Henrique, M.A.; Maranhão, L.J.C.D.N.; Vinhas, G.M.; Silva, K.K.d.O.S.; Costa, A.F.d.S.; et al. Design of a naturally dyed and waterproof biotechnological leather from reconstituted cellulose. *J. Funct. Biomater.* **2022**, *13*, 49. [CrossRef]
34. *ISO 20200:2015*; Plastics—Determination of the Degree of Disintegration of Plastic Materials Under Simulated Composting Conditions in a Laboratory-Scale Test. ISO: Geneva, Switzerland, 2015.
35. Jumaidin, R.; Diah, N.A.; Ilyas, R.A.; Alamjuri, R.H.; Yusof, F.A.M. Processing and characterisation of banana leaf fibre reinforced thermoplastic cassava starch composites. *Polymers* **2021**, *13*, 1420. [CrossRef]
36. Tureck, B.C.; Hackbarth, H.G.; Neves, E.Z.; Garcia, M.C.F.; Apati, G.P.; Recouvreux, D.O.S.; Pezzin, A.P.T.; Schneide, A.L.S. Obtaining and characterization of bacterial cellulose synthesized by *Komagataeibacter hansenii* from alternative sources of nitrogen and carbon. *Rev. Matéria* **2021**, *26*, e13092. [CrossRef]
37. Adamopoulou, V.; Bekatorou, A.; Brinias, V.; Michalopoulou, P.; Dimopoulos, C.; Zafeiropoulos, J.; Petsi, T.; Koutinas, A.A. Optimization of bacterial cellulose production by *Komagataeibacter sucrofermentans* in synthetic media and agrifood side streams supplemented with organic acids and vitamins. *Bioresour. Technol.* **2024**, *398*, 130511. [CrossRef] [PubMed]
38. Thongsuk, K.; Tippayasak, U.; Sukkasem, T.; Naloka, K.; Puangsin, B.; Chonudomkul, D.; Yakushi, T.; Theeragool, G. Production of probiotic bacterial cellulose with improved yield, mechanical properties, and antibacterial activity from cost-effective coculture and mixed-culture fermentation in coconut water by *Komagataeibacter xylinus* MSKU 12. *Int. J. Biol. Macromol.* **2025**, *291*, 139083. [CrossRef]
39. Skaradziński, G.; Janek, T.; Śliwka, P.; Skaradzińska, A.; Łaba, W. Statistical optimization of bacterial cellulose production and its application for bacteriophage immobilization. *Int. J. Mol. Sci.* **2025**, *26*, 6059. [CrossRef]
40. Bektas, I.; Yildirim, N.B. Molecular Characterization of bacterial cellulose producing *bacillus* strains isolated from soil. *J. Basic Microbiol.* **2025**, *65*, e70026. [CrossRef]
41. Jing, S.; Wu, L.; Siciliano, A.P.; Chen, C.; Li, T.; Hu, L. The critical roles of water in the processing, structure, and properties of nanocellulose. *ACS Nano* **2023**, *17*, 22196–22226. [CrossRef] [PubMed]
42. Srivastava, S.; Mathur, G. Bacterial Cellulose: A multipurpose biomaterial for manmade world. *Curr. Appl. Sci. Technol.* **2022**, *23*, 1–19. [CrossRef]
43. Cielecka, I.; Ryngajłło, M.; Maniukiewicz, W.; Bielecki, S. Highly stretchable bacterial cellulose produced by *Komagataeibacter hansenii* SI1. *Polymers* **2021**, *13*, 4455. [CrossRef]
44. Kalyoncu, E.E.; Peşman, E. Bacterial cellulose as reinforcement in paper made from recycled office waste pulp. *BioResources* **2020**, *15*, 8496–8514. [CrossRef]
45. Monteiro, M.K.S.; de Oliveira, V.R.L.; dos Santos, F.K.G.; Leite, R.H.d.L.; Aroucha, E.M.M.; da Silva, R.R.; Silva, K.N.d.O. Analysis of water barrier, mechanical and thermal properties of nanocomposites based on cassava starch and natural clay or modified by anionic exchange. *Mater. Res.* **2018**, *20*, 69–76. [CrossRef]
46. Provin, A.P.; dos Reis, V.O.; Hilesheim, S.E.; Bianchet, R.T.; Dutra, A.R.A.; Cubas, A.L.V. Use of bacterial cellulose in the textile industry and the wettability challenge—A review. *Cellulose* **2021**, *28*, 8255–8274. [CrossRef]
47. Asim, N.; Badiei, M.; Mohammad, M. Recent advances in cellulose-based hydrophobic food packaging. *Emergent Mater.* **2021**, *5*, 703–718. [CrossRef]
48. Gorrasi, G. Progress in barrier packaging materials: Bio-based nanocomposites as barrier materials for food packaging applications. In *Progress in Nanomaterials for Food Packaging*; Future Science Ltd.: London, UK, 2014; pp. 20–33. [CrossRef]
49. Sahu, R.; Khokhar, D. Evaluation of Water Vapour Permeability of Some Food Grain Packaging Materials. *J. Sci. Res. Rep.* **2024**, *30*, 558–563. [CrossRef]
50. Huang, K.; Maltais, A.; Wang, Y. Enhancing water resistance of regenerated cellulose films with organosilanes and cellulose nanocrystals for food packaging. *Carbohydr. Polym. Technol. Appl.* **2023**, *6*, 100391. [CrossRef]
51. Sapna; Sharma, C.; Pathak, P.; Yadav, S.P.; Gautam, S. Potential of emerging "all-natural" edible coatings to prevent post-harvest losses of vegetables and fruits for sustainable agriculture. *Prog. Org. Coat.* **2024**, *193*, 108537. [CrossRef]
52. Pashova, S. Application of plant waxes in edible coatings. *Coatings* **2023**, *13*, 911. [CrossRef]
53. Liyanapathiranage, A.; Dassanayake, R.S.; Gamage, A.; Karri, R.R.; Manamperi, A.; Evon, P.; Jayakodi, Y.; Madhujith, T.; Merah, O. Recent developments in edible films and coatings for fruits and vegetables. *Coatings* **2023**, *13*, 1177. [CrossRef]
54. Gu, X.; Du, L.; Meng, Z. Comparative study of natural wax-based W/O emulsion gels: Microstructure and macroscopic properties. *Food Res. Int.* **2023**, *165*, 112509. [CrossRef] [PubMed]

55. Naqash, S.; Naqash, F.; Fayaz, S.; Khan, S.; Dar, B.N.; Makroo, H.A. Application of Natural Antimicrobial Agents in Different Food Packaging Systems and Their Role in Shelf-life Extension of Food: A Review. *J. Packag. Technol. Res.* **2022**, *6*, 73–89. [CrossRef]
56. De Sousa, R.B.; Pinesso, G.; Diedrichs, R.R.; Da Silva, C.C.; Macêdo, L.P.R. Bacterial cellulose: A multifunctional platform for biomedical applications. *J. Mater. Sci. Technol. Res.* **2024**, *11*, 75–83. [CrossRef]
57. Popa, L.; Ghica, M.V.; Tudoroiu, E.-E.; Ionescu, D.-G.; Dinu-Pîrvu, C.-E. Bacterial cellulose—A remarkable polymer as a source for biomaterials tailoring. *Materials* **2022**, *15*, 1054. [CrossRef] [PubMed]
58. Zafeer, M.K.; Prabhu, R.; Rao, S.; Mahesha, G.; Bhat, K.S. Mechanical characteristics of sugarcane bagasse fibre reinforced polymer composites: A review. *Cogent Eng.* **2023**, *10*, 2200903. [CrossRef]
59. Otálora González, C.M.; Alvarez Castillo, E.; Flores, S.; Gerschenson, L.N.; Bengoechea, C. Effect of plasticizer composition on the properties of injection molded cassava starch-based bioplastics. *Food Packag. Shelf Life* **2023**, *40*, 101218. [CrossRef]
60. Jiménez-Rosado, M.; Bouroudian, E.; Perez-Puyana, V.; Guerrero, A.; Romero, A. Evaluation of different strengthening methods in the mechanical and functional properties of soy protein-based bioplastics. *J. Clean. Prod.* **2020**, *262*, 121517. [CrossRef]
61. Saputri, C.A.; Julyatmojo, F.A.; Harmiansyah; Febrina, M.; Mahardika, M.; Maulana, S. Characteristics of bioplastics prepared from cassava starch reinforced with banana bunch cellulose at various concentrations. *IOP Conf. Ser. Earth Environ. Sci.* **2024**, *1309*, 012006. [CrossRef]
62. Darmenbayeva, A.; Zhussipnazarova, G.; Rajasekharan, R.; Massalimova, B.; Zharlykapova, R.; Nurlybayeva, A.; Mukazhanova, Z.; Aubakirova, G.; Begenova, B.; Manapova, S.; et al. Applications and Advantages of Cellulose–Chitosan Biocomposites: Sustainable Alternatives for Reducing Plastic Dependency. *Polymers* **2024**, *17*, 23. [CrossRef]
63. Akhrib, S.; Djellali, S.; Haddaoui, N.; Karimian, D.; Carraro, M. Biocomposites and Poly(lactic acid) in Active Packaging: A Review of Current Research and Future Directions. *Polymers* **2025**, *17*, 3. [CrossRef]
64. Briassoulis, D.; Dejean, C.; Picuno, P. Critical Review of Norms and Standards for Biodegradable Agricultural Plastics Part II: Composting. *J. Polym. Environ.* **2010**, *18*, 364–383. [CrossRef]
65. Rudnik, E. Composting methods and legislation. In *Compostable Polymer Materials*; Elsevier: Amsterdam, The Netherlands, 2019; pp. 127–161. [CrossRef]
66. Schutz, G.F.; de Ávila Gonçalves, S.; Alves, R.M.V.; Vieira, R.P. A review of starch-based biocomposites reinforced with plant fibers. *Int. J. Biol. Macromol.* **2024**, *261*, 129916. [CrossRef]
67. Pirog, T.P. Synergism of antimicrobial activity of antibiotics with biocides of natural origin. *Biotechnol. Acta* **2024**, *17*, 5–19. [CrossRef]
68. Pantić, M.; Nowak, M.; Lavrič, G.; Knez, Ž.; Novak, Z.; Zizovic, I. Enhancing the properties and morphology of starch aerogels with nanocellulose. *Food Hydrocoll.* **2024**, *156*, 110345. [CrossRef]
69. Meza-Contreras, J.C.; Manriquez-Gonzalez, R.; Gutiérrez-Ortega, J.A.; Gonzalez-Garcia, Y. XRD and solid state 13C-NMR evaluation of the crystallinity enhancement of 13C-labeled bacterial cellulose biosynthesized by *Komagataeibacter xylinus* under different stimuli: A comparative strategy of analyses. *Carbohydr. Res.* **2018**, *461*, 51–59. [CrossRef]
70. Fernández, N.L.; Yamul, D.K.; Navarro, A.S. Physicochemical and mechanical properties of cassava starch films containing honey and glycerol as co-plasticisers. *Int. J. Food Sci. Technol.* **2025**, *60*, vvae017. [CrossRef]
71. de Almeida, N.T.; Pereira, A.L.S.; Barros, M.d.O.; Mattos, A.L.A.; Rosa, M.d.F. Enhancing starch film properties using bacterial nanocellulose-stabilized pickering emulsions. *Polymers* **2024**, *16*, 3346. [CrossRef]
72. Tacha, S.; Somord, K.; Rattanawongkun, P.; Intatha, U.; Tawichai, N.; Soykeabkaew, N. Bio-nanocomposite foams of starch reinforced with bacterial nanocellulose fibers. *Mater. Today Proc.* **2023**, *75*, 119–123. [CrossRef]
73. Phiri, R.; Mavinkere Rangappa, S.; Siengchin, S. Sugarcane bagasse for sustainable development of thermoplastic biocomposites. *Ind. Crops Prod.* **2024**, *222*, 120115. [CrossRef]
74. Sánchez, J.H.; Fajardo, M.E.; Quintana, G.C. Viscoelastic Properties of pulp suspensions of bleached sugarcane bagasse: Effects of consistency and temperature. *BioResources* **2016**, *11*, 8355–8363. [CrossRef]
75. Semple, K.E.; Zhou, C.; Rojas, O.J.; Nguegang Nkeuwa, W.; Dai, C. Moulded pulp fibers for disposable food packaging: A state-of-the-art review. *Food Packag. Shelf Life* **2022**, *33*, 100908. [CrossRef]
76. Alokika; Anu; Kumar, A.; Kumar, V.; Singh, B. Cellulosic and hemicellulosic fractions of sugarcane bagasse: Potential, challenges and future perspective. *Int. J. Biol. Macromol.* **2021**, *169*, 564–582. [CrossRef] [PubMed]
77. Garcia, M.C.; Elias, T.M.; Ribeiro, K.O.; Soares Júnior, M.S.; Caliari, M. Microbiological and physicochemical profiles of the sour cassava starch and bagasse obtained from cassava agroindustry. *Food Sci. Technol.* **2018**, *39*, 803–809. [CrossRef]
78. Travalini, A.P.; Prestes, E.; Pinheiro, L.A.; Demiate, I.M. Extraction and characterization of nanocrystalline cellulose from cassava bagasse. *J. Polym. Environ.* **2018**, *26*, 789–797. [CrossRef]
79. Widiarto, S.; Pramono, E.; Suharso; Rochliadi, A.; Arcana, I.M. Cellulose nanofibers preparation from cassava peels via mechanical disruption. *Fibers* **2019**, *7*, 44. [CrossRef]
80. Liu, C.; Luan, P.; Li, Q.; Cheng, Z.; Sun, X.; Cao, D.; Zhu, H. Biodegradable, hygienic, and compostable tableware from hybrid sugarcane and bamboo fibers as plastic alternative. *Matter* **2020**, *3*, 2066–2079. [CrossRef]

81. Laavanya, D.; Shirkole, S.; Balasubramanian, P. Current challenges, applications and future perspectives of SCOBY cellulose of Kombucha fermentation. *J. Clean. Prod.* **2021**, *295*, 126454. [CrossRef]
82. Gagliardi, T.R.; Nascimento, A.d.F.; Valencia, G.A. Kombucha bacterial cellulose: A promising biopolymer for advanced food and nonfood applications. *Foods* **2025**, *14*, 738. [CrossRef]
83. Zhong, C. Industrial-scale production and applications of bacterial cellulose. *Front. Bioeng. Biotechnol.* **2020**, *8*, 605374. [CrossRef]